Biointerface Research in Applied Chemistry
Open-Access Journal (ISSN: 2069-5837)

Article
Volume 14, Issue 1, 2024, 19
https://doi.org/10.33263/BRIAC141.019

Molecular Docking Analysis and Spectroscopic Investigations of Cobalt(III), Copper(II) and Nickel(II) Complexes of Schiff Base Ligand Derived From Metformin: Evaluation of DNA Binding, Antioxidant and Antimicrobial Activities

Prema Mahadeva [1], Hosaere D. Revanasiddappa [1,*]

[1] Department of Studies in Chemistry, University of Mysore, Manasagangotri, Mysuru-570006, India
[*] Correspondence: hdrevanasiddappa@yahoo.com;

Scopus Author ID 7004879365
Received: 24.04.2023; Accepted: 28.05.2023; Published: 2.02.2024

Abstract: Herein, computational molecular docking, UV-visible, and fluorescence spectroscopic techniques have been used to explore the DNA, p53 cancer mutant protein and Cu, Zn-SOD binding interaction of the ligand (HL) and its Co (III), Cu (II) and Ni(II) complexes$[Co(HL)_2(H_2O)_2].3H_2O$ (C-1); $[Cu(HL)_2(H_2O)_2].2H_2O$ (C-2) and $[Ni(HL)_2(H_2O)_2]. 4H_2O$ (C-3). The compounds were further tested for antimicrobial activities. The DNA binding studies were carried out under physiological conditions of pH(7.4) and temperature (34 ˚C). The spectral experiments revealed that the metal complexes showed comparatively greater binding constant values. Docking analysis depicted that the ligand HL(L-2) interacted with DNA via intercalation, while its complexes showed a mixed mode of interactions, and the Cu (II) complex displayed a more binding affinity with DNA and Cu, Zn-SOD enzyme. The copper complex showed good antibacterial activity against the tested strains. The Cu and Ni complexes exhibited greater antioxidant activities with lower IC50 values.

Keywords: Fluorescence, CT-DNA, BSA, molecular docking, enhancement, quenching

1. Introduction

Schiff base is named after Hugo Schiff [1-3]. Schiff bases are also called imines and are obtained by condensing aldehyde or ketone with amine. They contain a characteristic azomethine group (C=N-) and are represented by the general formulae R1R2C=NR3. Usually, aromatic aldehydes are preferred over aliphatic aldehydes due to the reason that aliphatic aldehydes are unstable and easily undergo polymerization. The condensation occurs in the presence of acid, base, or heating [4]. The acid-catalyzed condensation involves the nucleophilic attack of the primary amine on the carbonyl center to give an unstable intermediate, carbinolamine. The acid-catalyzed dehydration of carbinolamine results in conversion to an N-substituted imine or Schiff base [5]. The availability of Schiff bases in many areas, such as biological systems and medicine itself, explains the scope of Schiff bases. In addition, imines are important intermediate and multipurpose starting materials for the synthesis of Mannich bases, indoles, and beta-lactam etc., The products of these reactions, along with Schiff bases, have been used for treating many diseases due to their biological activity. Schiff bases contain donor atoms [N,O,S] which makes them biologically active and

excellent chelators of metal [6]. A large number of different Schiff bases have been used as cation carriers in potentiometric sensors as they have shown excellent selectivity, sensitivity, and stability for specific metal ions such as Ag(I), Al(III), Co(III), Gd(II), Hg(II), Ni(II), Pb(II), Y(III) and Zn(II). The azomethine group of Schiff base plays a vital role in elucidating the mechanism of certain reactions of biological systems, such as transamination and racemization [7]. Schiff bases are active against a wide range of organisms, including bacteria and fungi [8]. The metal complexes have been an attractive area of research in view of their significance as bio-mimetic catalysts in the process of oxygenation. The wide usage of Schiff base ligands is due to their properties, such as stability and solubility in common solvents [9].

The oxygen and nitrogen-containing Schiff base metal complexes continues to attract researchers' attention. These ligands are known to coordinate with metal atoms in different ways under different reaction conditions [10-11]. Schiff base metal complexes have important applications in medicinal Chemistry, Medical Science. Transition metal complexes have binding capacity with amino acids. Metal ions provide stability of the complex by delocalization of electrons of the ligand by ligand and chelation and enhance their activity [12-13]. Transition metal complexes with Schiff base ligands have been extensively investigated as antimicrobial, anticancer agents [14].

2. Materials and Methods

2.1. Materials.

Metformin, 3-phenoxy benzaldehyde, ethanol, DMSO, Tris HCl buffer, calf thymus DNA (highly polymerized, stored at 4 ˚C), CT- DNA, DPPH, and BHA were purchased from Sigma Corp. and they were used as supplied.

2.2. Methods and Instrumentation.

The melting point determination was uncorrected in an open capillary tube using a precision digi-melting point apparatus. Mass spectra of synthesized compounds were recorded using 2010 EV LCMS Shimadzu spectrometer. The ^{1}H and ^{13}C NMR spectra were recorded using VNMRS-400 “Agilent–NMR” spectrophotometer, and chemical shifts are given in ppm with residual DMSO as reference. FT-IR spectra were recorded on a Perkin-Elmer Spectrum Version 10.03.09 spectrophotometer in the range 4000-400 cm^{-1}. Microanalysis (C, H, N, O, and M) was performed on a Perkin-Elmer analyzer. UV-visible spectra were recorded using DU 730 Spectrophotometer, S/N 1333105, Instrument version: 1.05, with a diode array detector. Fluorescence spectra were measured on a Varioskan Flash (4.00.53 Thermo-scientific USA) with 96 well plates. The excitation and emission slits were set at 5 nm each. The wavelength increment was set at 2 nm. Electron spin resonance (ESR) spectra were recorded using JOEL JES-TE100 ESR Spectrometer in DMSO solution at LNT in the solid state on X-band at a frequency of 9.13 GHz under the magnetic field of 300 mT.

2.2.1. Synthesis of ligand [HL].

The ligand HL was synthesized by 1:1 condensation of metformin with 3-Phenoxy benzaldehyde. Add a solution of metformin (0.15g) in 8 mL of hot ethanol, 3-phenoxy benzaldehyde (0.17g) in 5 mL ethanol was refluxed for 5 h at 70˚C. After cooling to room temperature, the white crystals were formed. The crystals were washed with ethanol and dried

in a desiccator. The progress of the reaction was monitored using TLC [n-hexane: ethyl acetate=8:2]. A pure synthesized compound was obtained from continuous recrystallization.

2.2.2. Synthesis of metal complexes [C-1, C-2 and C-3].

The ligand (HL, 2.0 mmol) was made dissolved in ethanol by heating and intensive stirring. To the warm suspension, the warm ethanol solution of cobalt(II)chloride hexahydrate (1.0mmol) was added dropwise. The resulting mixture was kept under reflux over a water bath for 4 h at 80˚C. The solvent was evaporated, and the obtained solid was directly used for further processing. Similarly, the complexes C-2 and C-3 were prepared using Copper(II)chloride dihydrate and Nickel(II)chloride heptahydrate.

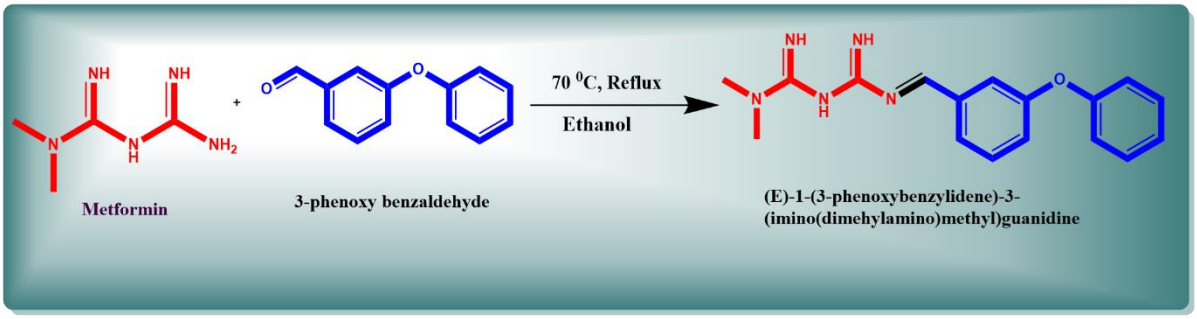

Scheme 1. Synthesis of Schiff base ligand (HL).

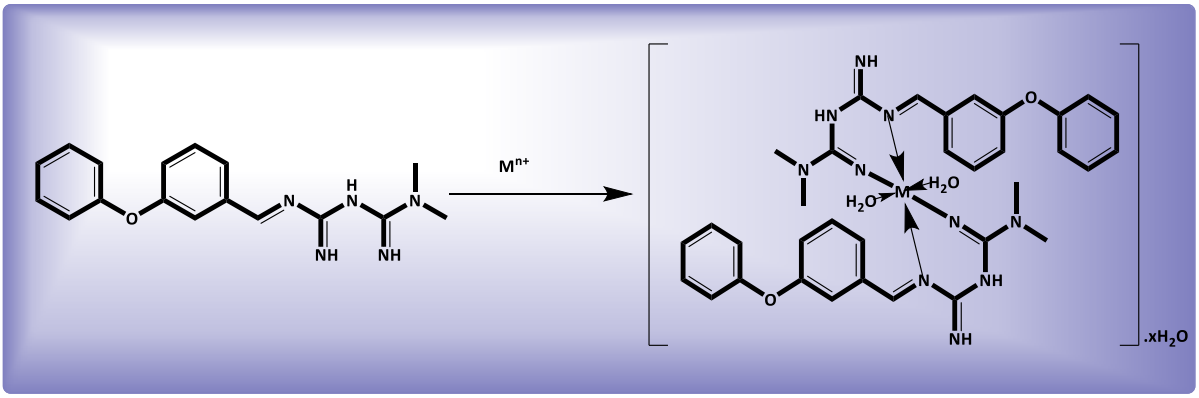

M= Co, Cu and Ni

Scheme 2. General scheme for the synthesis of metal complexes [C-1 to C-3].

2.3. Bioassay studies.

2.3.1. Molecular docking methodology.

Crystal structure of DNA (1BNA), p53 cancer mutant protein (4L09), and Cu, Zn-SOD (1CB4) were downloaded from the protein data bank (www.rcsb.org) and used for docking studies. The synthesized compounds were drawn in chem draw software, and energy minimization was computed by PyRx. The DNA, p53 cancer mutant protein, and Cu, Zn-SOD were prepared in Biovia discovery studio by adding hydrogen to the polar atoms, and the metal ions' valency was optimized [15]. The water molecules and substrate were deleted. A grid for DNA [with the dimension (22.7058 x 23.8346 x 38.3763 A˚ for HL; 22.2376 x 23.7867 x 37.3423 A˚ for C-1; 23.2378 x 23.9765 x 38.4598 A˚ for C-2; 22.4991 x 23.1487 x 37.8898 A˚ for C-3,

respectively), for p53 cancer mutant protein (with the dimension of 71.1348 x 90.0226 x 25.0000A˚ for HL; 72.2376 x 91.1022 x 26.0123 A˚ for C-1; 73.1587 x 93.8976 x 28.4513A˚ for C-2; 72.5499 x 91.2987 x 26.2365 A˚ for C-3, respectively) and for Cu,Zn-SOD (with the dimension (70.6320 x 51.6335x 18.4356A˚ for HL; 71.1223 x 52.1122 x 19.2123 A˚ for C-1; 72.5367 x 51.8987 x 18.8978 A˚ for C-2; 72.5379 x 52.2348 x 19.2485 A˚ for C-3, respectively) were prepared. The compounds were evaluated based on glide scoring[16].

2.3.2. Spectrophotometric titrations.

Absorption spectra were recorded on a UV-visible spectrophotometer using 3 mL quartz cuvettes. The DNA binding experiments were carried out at physiological pH (7.4) and temperature (34˚C) by keeping the constant complex concentration with varied concentrations of CT-DNA from 1 – 7 µM. The concentration of the stock solution of CT-DNA was fixed as 10-4 M and UV-visible spectra were recorded. The binding constant was calculated using the eq (1)

$$\frac{[DNA]}{\epsilon a-\epsilon b}=\frac{[DNA]}{\epsilon b-\epsilon f}+\frac{1}{Kb(\epsilon b-\epsilon f)} \quad (1)$$

Where [DNA] is the concentration of CT-DNA. ϵa is the apparent extinction co-efficient and ϵf is the extinction coefficient of the free complex in the absence of DNA, ϵb is the extinction coefficient of the complex with bound DNA, and Kb is the binding constant [17].

2.3.3. Antioxidant activity.

The free radical scavenging activity of each sample was measured by 1,1-diphenyl-2-picrylhydrazyl assay. The methanolic solution of DPPH (0.2mM) was prepared and incubated for 2 hours prior to the analysis [18]. 2mg of the ligand (HL) and its metal complexes were dissolved in methanol. 1ml of DPPH was added to different volumes of ligand and metal complexes and made up to 4 mL using a solvent. The samples were stored in the dark at room temperature, and after 30 minutes, the absorbance was measured at 517 nm using BHA as standard and control [19]. DPPH scavenging activity was calculated using the eq (2)

$$\% \text{ DPPH scavenging} = \frac{Ac-As}{Ac} x\ 100 \quad (2)$$

Where, Ac –absorbance of the control; As- absorbance of the sample

The lower absorbance of the reaction mixture indicates higher free radical scavenging activity [20]

2.3.4. Antimicrobial assay.

The synthesized compounds were screened for their antimicrobial activity against Gram –ve bacteria as *Escherichia coli* (MTCC 443) and Gram +ve bacterial strains as *Staphylococcus aureus* (MTCC 3160), *Bacillus subtilis* (MTCC 121), fungal strains are *Aspergillus niger* (ATCC 6275) and *Candida albicans* (ATCC 10231), standard antibiotic amoxicillin (25mg) and antifungal fluconazole (25mg) served as positive control. The microbes were tested regarding minimum inhibitory concentration (MIC) using a serial plate dilution assay [21]. Microbial cultures were incubated at 34˚C for a day in the case of bacteria, and 24 h for fungi, respectively. Mueller-Hinton broth of bacteria(100µL) was pipette into each well, and 10 µL suspension of the pathogens was then added. 4% DMSO solution was used as a negative control to monitor the sterility of the sample and to assess the antimicrobial influence of the solvent. Zone of inhibition was measured, and MIC was obtained by double-fold serial dilution in liquid

media containing varying concentrations of test samples from 1 to 1000 µg/mL. Bacterial growth was measured by the turbidity of the culture after 18h. McFarland Standard 0.5 was used as the turbidity standard.

3. Results and Discussion

3.1. chemistry.

A new N, N donor bidentate bioactive ligand (HL) and its Co(III), Cu(II), and Ni(II) complexes were prepared, followed by the literature methods. The micro-elemental analysis for C, H, N, O, and M and the molecular weight of the complexes were in good agreement with the proposed structure of the complexes [22,23]. Analytical data obtained were summarized, and the results obtained are reliable with those calculated for the proposed formulae. The synthesized compounds were stable, non-hygroscopic, and soluble in organic solvents such as ethanol, DMF, and DMSO. The analytical data is depicted in Table-1. An outline of the proposed structure of HL and the complexes are shown in Scheme-1 and Scheme-2[24].

Table 1. Physical properties of the synthesized ligand(Hl) and its metal complexes C-1, C-2, and C-3.

Compound	M.W. (g/mol)	color	M.P. ˚C	% Yield	M.L.	Elemental analysis				
						C	H	N	O	M
HL	309	white	188	89	-	66	6.19	22.64	5.17	-
C-1	764	Blue	149	91	1:2	54.27	5.89	18.61	12.75	8.45
C-2	753	Green	204	84	1:2	53.45	5.80	18.33	14.66	7.72
c-3	782	Pale green	161	82	1:2	53.48	5.81	18.34	14.67	7.68

3.2. FT-IR spectral analysis.

The IR spectrum of the ligand (HL) is compared with that of metal complexes to investigate the binding mode between the ligand and the metal ions. The characteristic bands in the IR spectrum of the synthesized HL and the metal complexes are listed in Table 2 and Fig 2. The band at 1689 is assigned to (C=N-) stretching frequency. The band at 3380 and 2855 cm^{-1} are due to the stretching of (-NH) and (-CH) groups, respectively. On complexation, the bands of the azomethine groups shift to lower wave number (1670, 1624, and 1602cm^{-1}) as compared to that of the imine ligand. Looking at the shifts and decrease in intensities before and after complexation indicates that these groups are involved in the complex formation. From the IR spectral data, it is known that HL behaves as a bidentate ligand. The IR spectral data are listed in Table 2 and shown in Fig 2 [25,26].

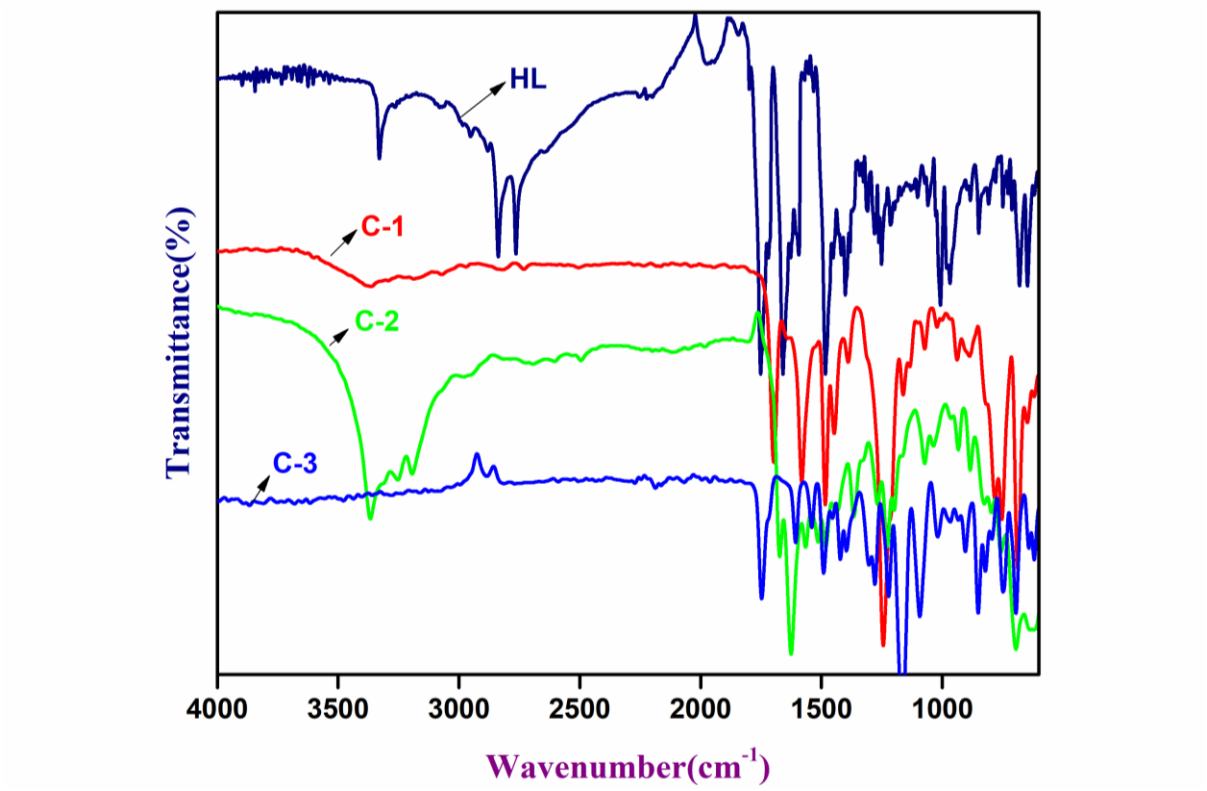

Figure 2. FT-IR spectra of HL and its metal complexes C-1, C-2 and C-3.

Table 2. FT-IR spectra of ligand (HL) and its metal complexes C-1 to C-3.

Compound	ν(C=N)	ν(N-H)	ν(C-H)	ν(N-N)	ν(C=C)	ν(C-O)	ν(M-N)
HL	1689	3380	2855	1125	1598	1289	-
C-1	1670	3090	2738	1041	1575	1241	673
C-2	1624	3189	2684	1051	1562	1225	691
C-3	1602	2999	2810	1089	1588	1251	696

3.3 UV/visible spectra.

The absorption spectra of HL and its metal complexes were recorded in dimethyl sulfoxide solution in the range 250-800nm. In the UV spectrum of the ligand, the absorption band at 258 and 328 nm corresponds to л-л* and n- л* transitions (Table 3, Fig 3). While the electronic spectrum of $[Co(L\text{-}2)_2(H_2O)_2].3H_2O$; $[Cu(L\text{-}2)_2(H_2O)_2].2H_2O$ and $[Ni(L\text{-}2)_2(H_2O)_2].4\ H_2O$ complexes displayed one band at 274, 287, and 276 nm are attributed to л-л* transitions, and the bands at 319, 336, 343 nm correspond to n- л* transition, and the absorption bands at 693, 601and 687nm correspond to d-d transitions, respectively. The C-2 and C-3 complexes showed peaks at 394 and 412 nm attributed to charge transfer transitions [27,28].

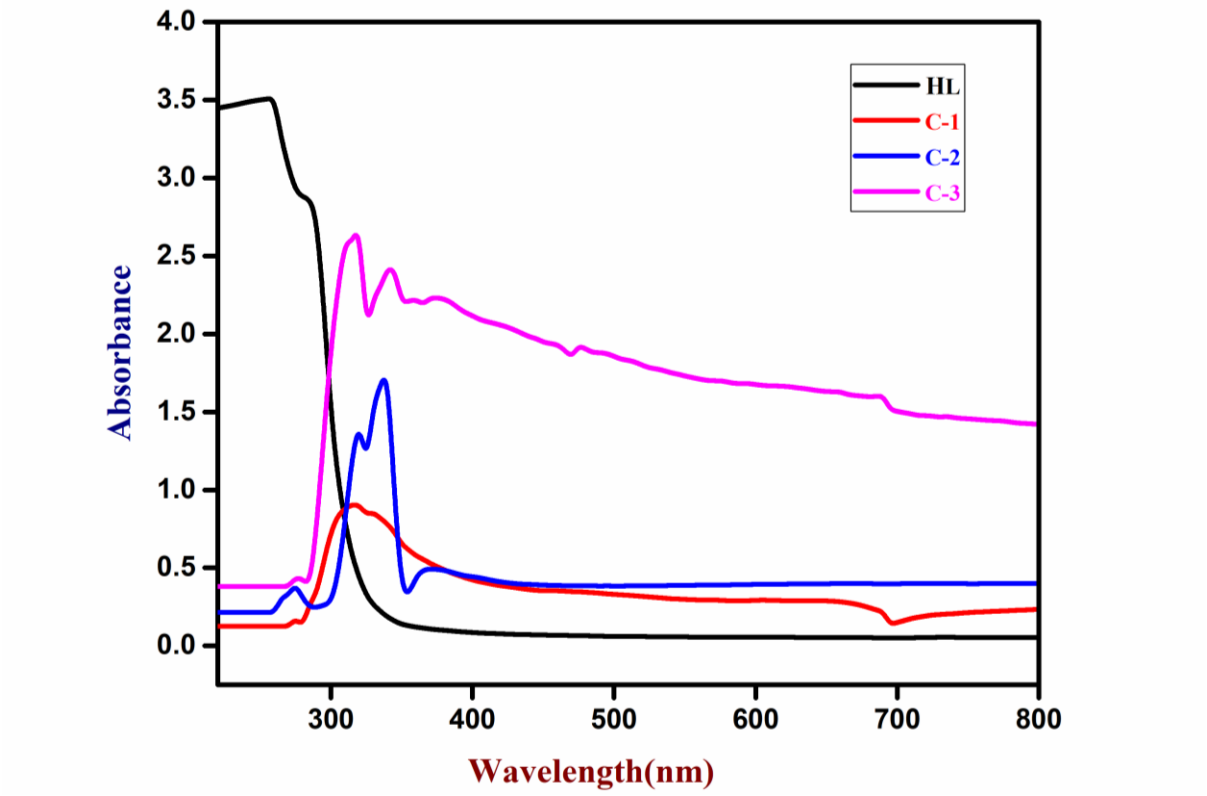

Figure 3. UV-Visible spectra of (HL) and its metal complexes C-1 to C-3.

Table 3. UV-Visible spectra of (L-2) and its metal complexes C-1 to C-3.

Compound	π-π*	n-π*	C-T transition	d-d transition
HL	258nm	328nm	-	-
C-1	274nm	319nm	-	693
C-2	287nm	336nm	394nm	601
C-3	276nm	343nm	412nm	687

3.4. NMR spectroscopy.

^{1}H spectra of HL were recorded in DMSO-d_6 and is given in Figure S-1. The hydrogen of the azomethine (C=N) group shows a singlet at 9.96 ppm. The multiple signals of Ar-H were observed between 6.81-7.67. The structure of the ligand was further evaluated using ^{13}C NMR. The signals at δ=149.49 ppm are attributed to the carbon of the azomethine group (C=N). The peaks observed between δ=110.6-157.2 ppm showed the aromatic ring carbons. The spectrum showed in Figure S-2 [29].

3.5. Mass spectroscopy.

The structure of the synthesized ligand (HL) and its metal complexes were confirmed through mass spectra. The mass spectrum of HL was shown in Figure S-3. The molecular ion peak is observed at m/z = 310[M-H], a molecular mass of the ligand (HL). The mass spectrum of the complexes showed molecular ion peaks at m/z= 765, 753, and 782 [M+1] confirmed the mass of the complexes C-1, C-2, and C-3, which are evident in Figures S-4, S-5, and S-6, respectively [30].

3.6. Thermo-gravimetric analysis.

The complexes (C-1 and C-3) have been subjected to a temperature program between the temperature range of 27 ℃ to 800 ℃ under inert temperature, with a heating rate of 10 ℃. [31]

The thermal degradation of the complex C-1 begins with the elimination of tthree water molecules at 60 ℃ to 165 ℃ with a weight loss of 7.04 % (calc.7.06 %). Another decomposition peak at 220 to 380 ℃ showed a weight loss of 85.58% (calc. 85.60%) as a result of the loss of coordinated organic moiety. Finally, the complex exhibited an exothermic peak at 390- 410 ℃ corresponds to thermal decomposition proceeded gradually with the formation of final residue CoO at 410 to 800 ℃ [32].

The decomposition of C-3complex has started with the breaking of the hydrogen bond of the water molecule with an endothermic peak at 59 ℃ followed by the loss of four water molecules with an endothermic peak at 70 -100 ℃ showing 9.12 % weight loss [calc 9.18%]. The DTA peaks were observed at 310 and 423℃ with 83.10 % weight loss [calc.83.18%]. It can be owed to the decomposition of two organic ligands. Oxidative thermal decomposition occurred in the range of 490 to 700 ℃ with an exothermic peak leaving NiO [33]. The TGA and DTA plots of complexes C-1 and C-3 are shown in Fig 4 and Fig 5, respectively.

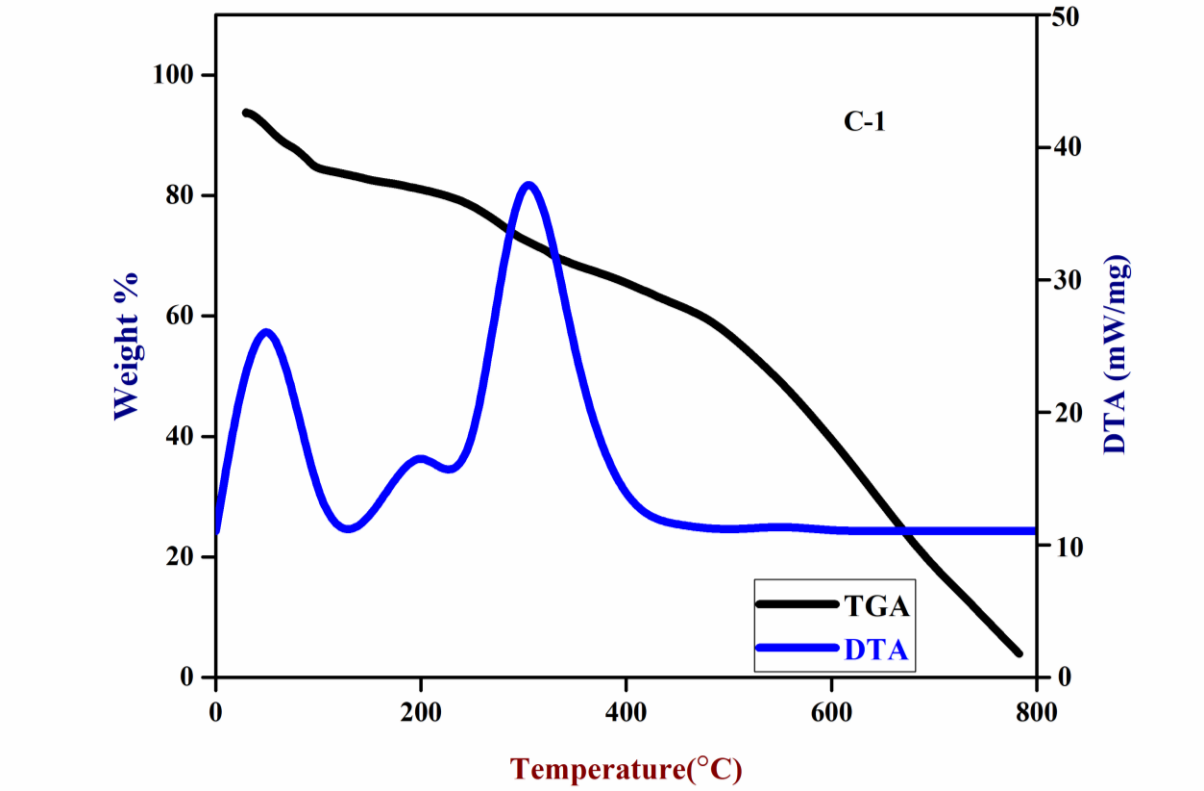

Figure 4. TGA and DTA plot of C-1 complex.

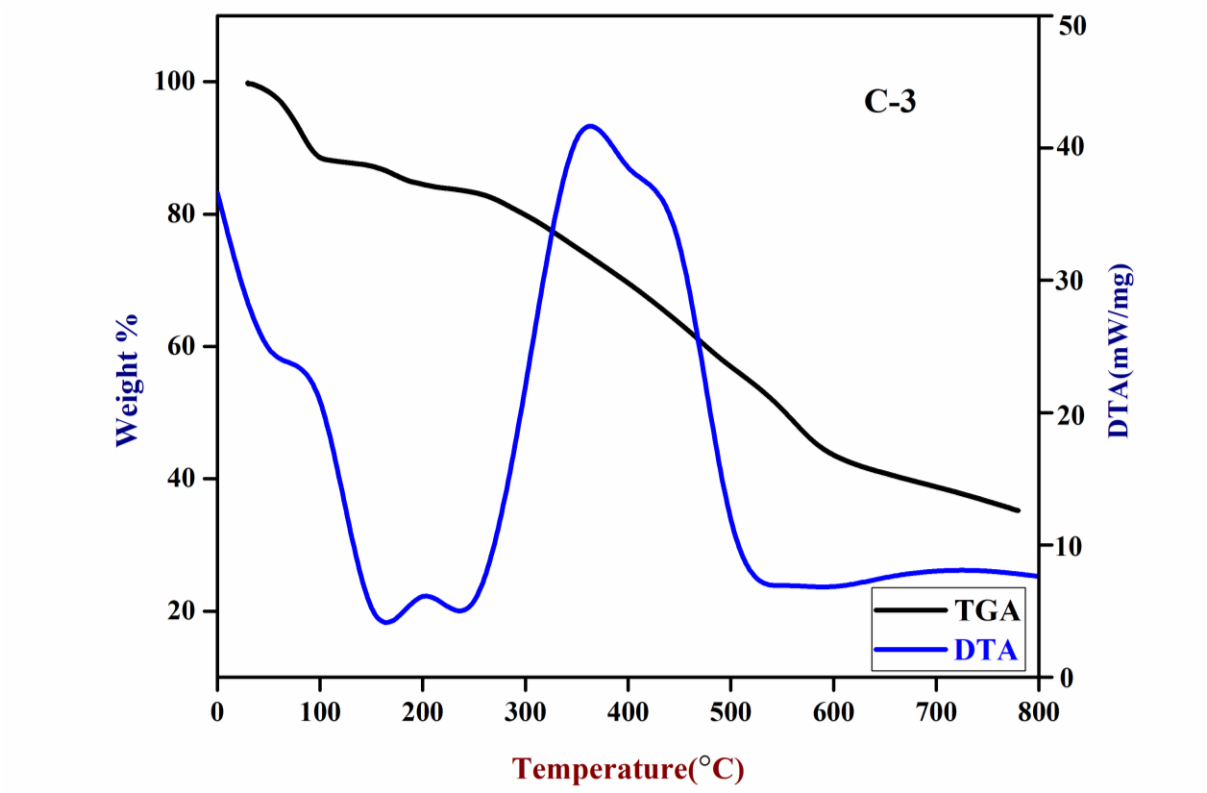

Figure 5. TGA and DTA plot of C-3 complex.

3.7. ESR Spectra.

The magnetically active copper metal center was investigated by ESR spectral analysis, and it was measured on the X-band at liquid nitrogen temperature using DMSO as a solvent. ESR spectra of copper complex, attributed to the coupling interaction of the copper nuclei with the unpaired electron; as a result, a single main band appeared in the spectra. The studies of the spectrum give $g\parallel$=2.104 and $g^{\perp}$ = 2.043. This clearly indicates that $g\parallel > g^{\perp}$ >2.0023 and the unpaired electron in Cu (II) reside in dx^2-dy^2 orbital and is the characteristic spectral feature for axial symmetry (Fig 6). The complex has tetragonally elongated geometry [34, 35].

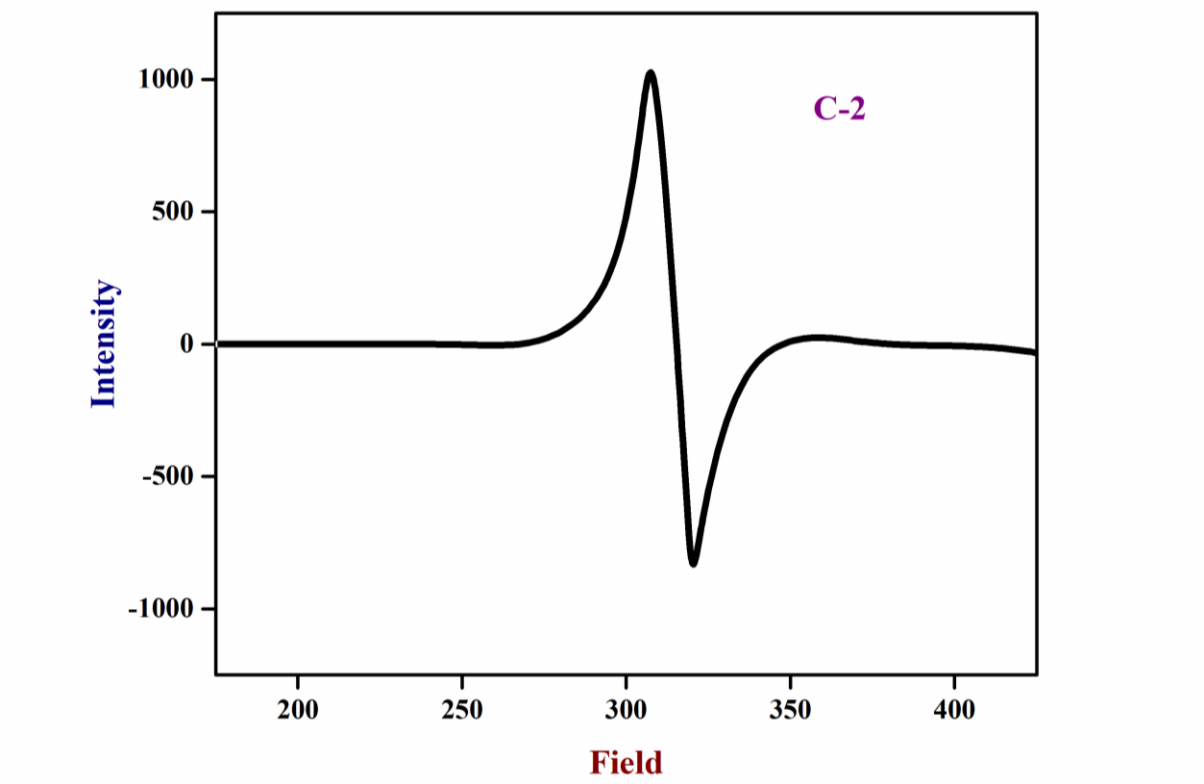

Figure 6. ESR spectrum of C-2 complex.

3.8. Molecular docking investigations.

It is a technique used to define the binding interaction sites available in the discovery studio visualizer. This calculation has been used to interpret how these proteins interact with small molecules [36]. The interaction of DNA(1BNA) and Cu, Zn-SOD(1CB4) with HL and its metal complexes C-1, C-2, and C-3 with docked energy parameters is shown in Table 4 and Fig 7a, 7b, 8a, 8b, 9a,9b, 10a and 10b respectively. These parameters infer that the C-2 complex will bind strongly with 1BNA [37]. The ligand (HL) and its metal complexes C-1, C-2, and C-3 interact with DNA with the binding energies of -6.5, -6.9, -7.4, and -7.0 kcal/mol, respectively. The interactions of HL and its metal complexes C-1, C-2, and C-3 with p53 cancer mutant protein with the binding scores of -8.0, -7.9, -8.3 and -8.1 kcal/mol and with Cu, Zn-SOD with the binding scores of -7.5, -7.8, -8.1and -7.9 kcal/mol, respectively. Docked compounds were analyzed based on hydrogen bonding, noncovalent and hydrophobic interactions between 1BNA, 4L09,1CB4, and the synthesized compounds. The docking investigations revealed that the copper complex interacts more efficiently with DNA, p53 cancer mutant protein, and hydrolase enzyme than other synthesized compounds. It showed the highest binding score with the p53 cancer mutant protein [38].

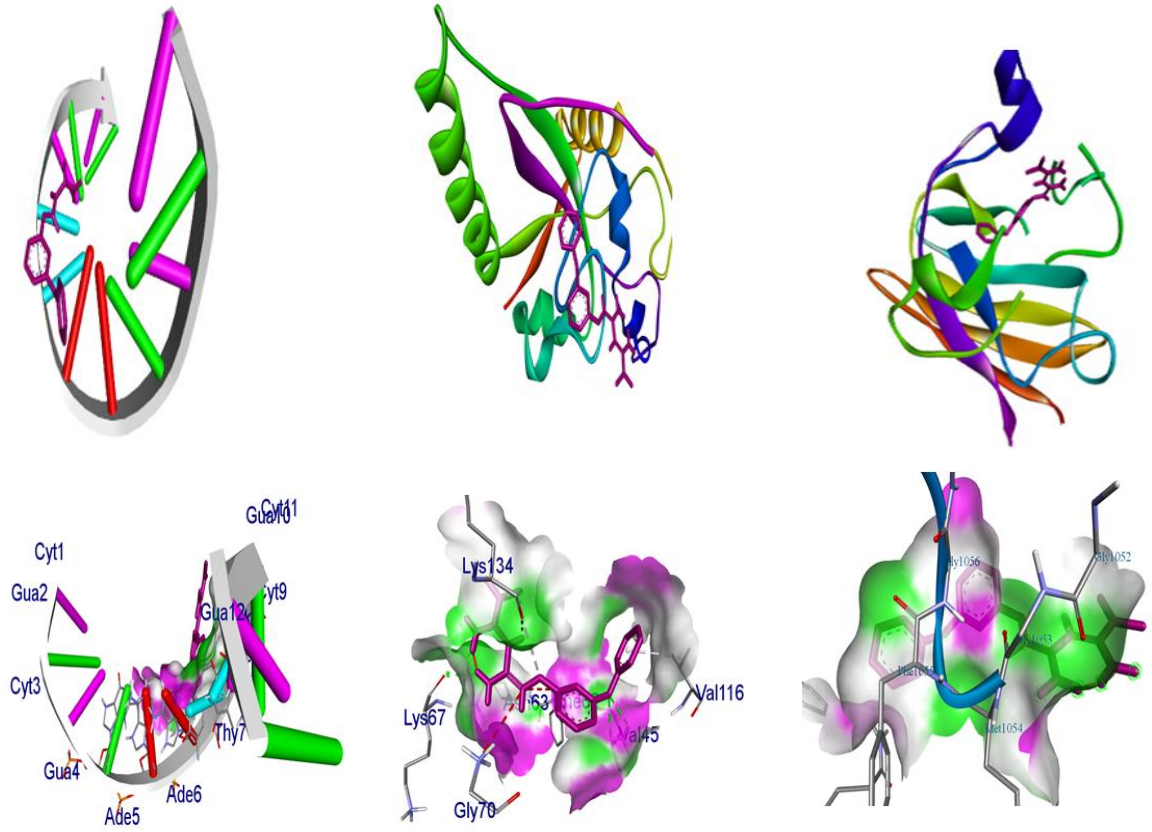

Figure 7. (a) Molecular docking of HL with 1BNA, 4L09, and 1CB4(above);**(b)** Active site aminoacid (1BNA, 4L09, and 1CB4) residues interactions with HL (below).

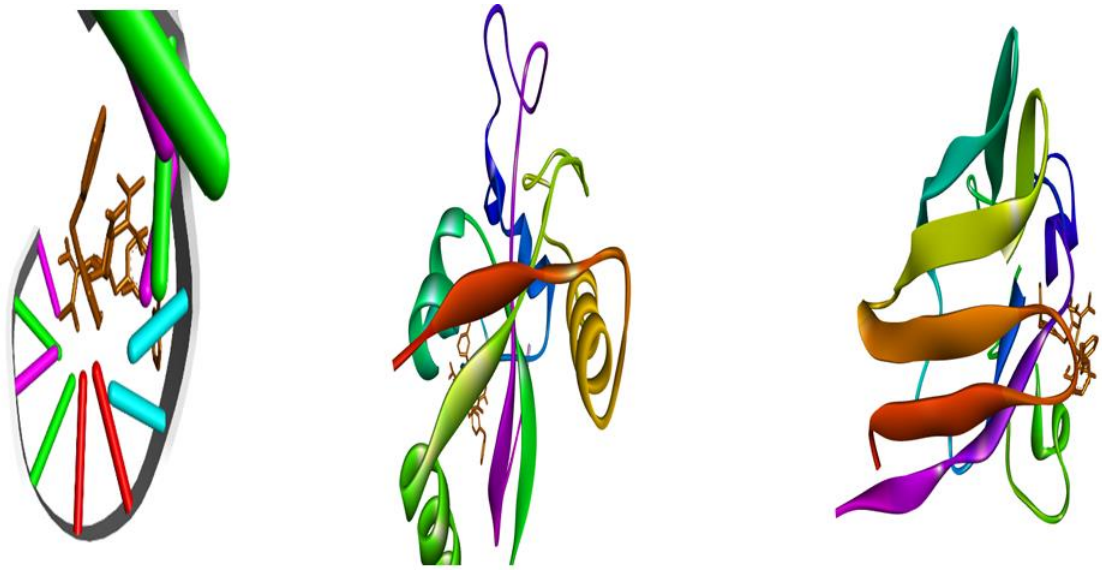

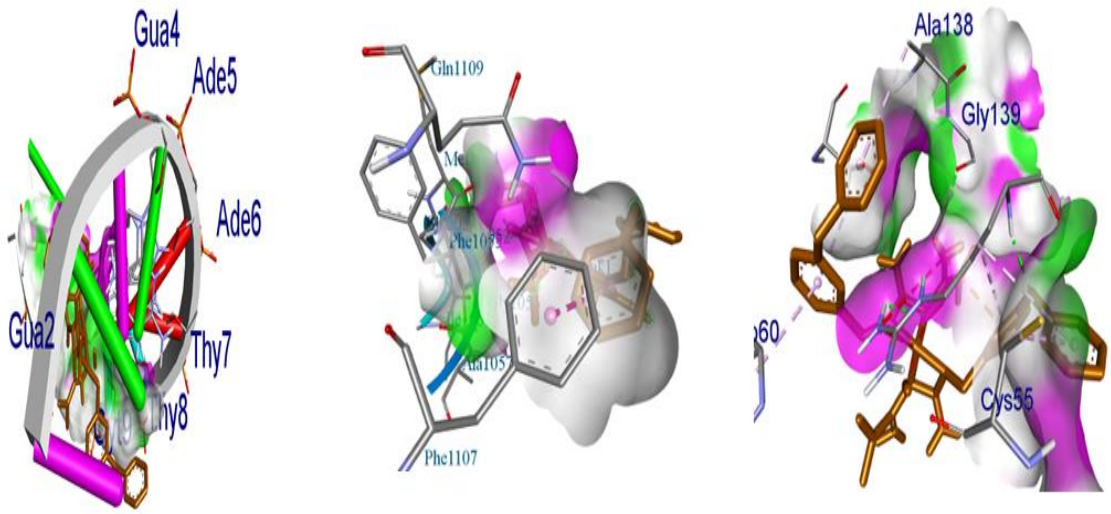

Figure 8. (a) Molecular docking of C-1 complex with 1BNA,4L09 and 1CB4 (above) **(b)** Active site amino acid (1BNA,4L09 and 1CB4) residues interaction with C-1 complex (below).

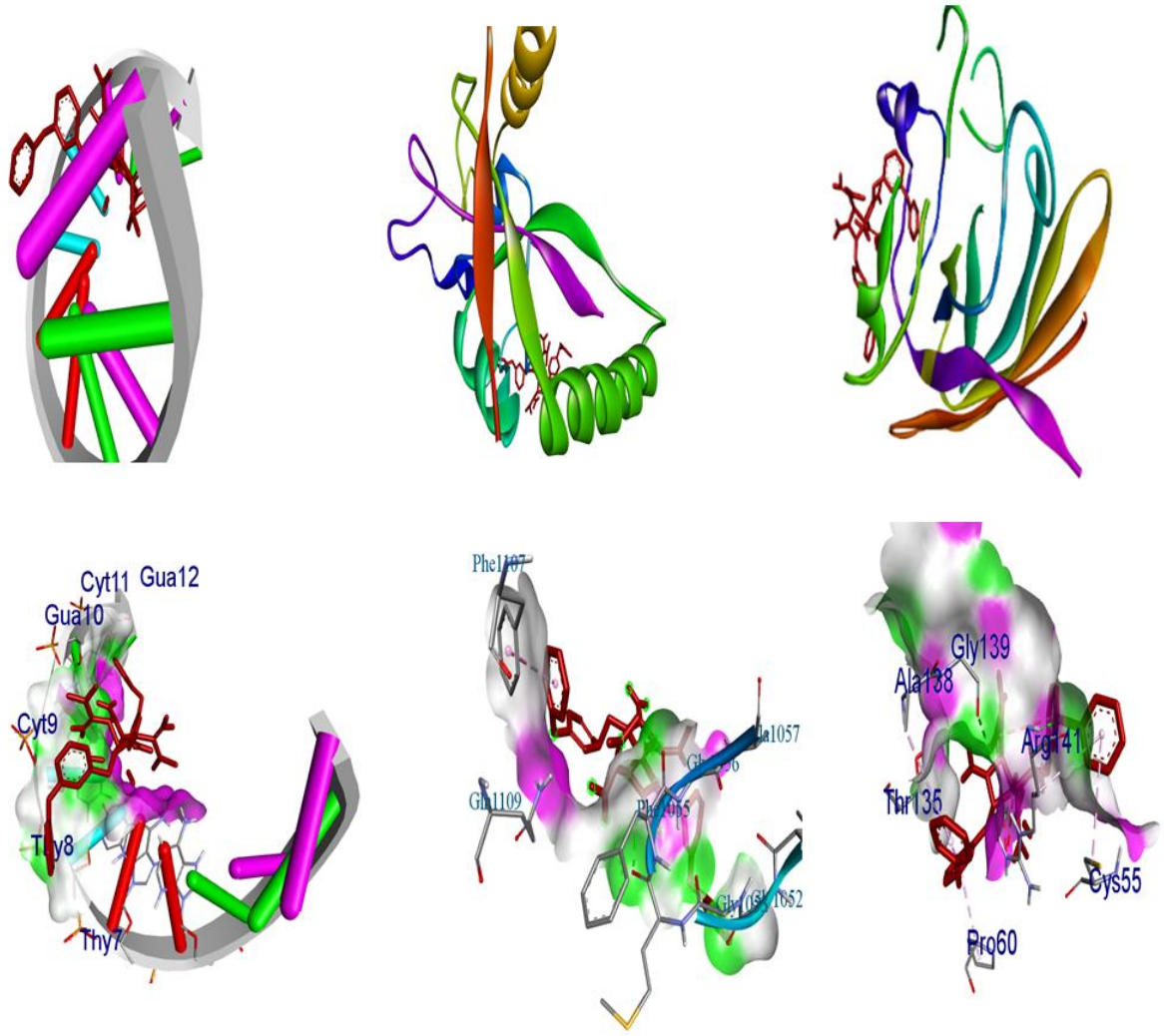

Figure 9.(a) Molecular docking of C-2 complex with 1BNA, 4L09 and 1CB4 (above); **(b)** Active site amino acid residue (1BNA, 4L09 and 1CB4) interactions with C-2 complex (below).

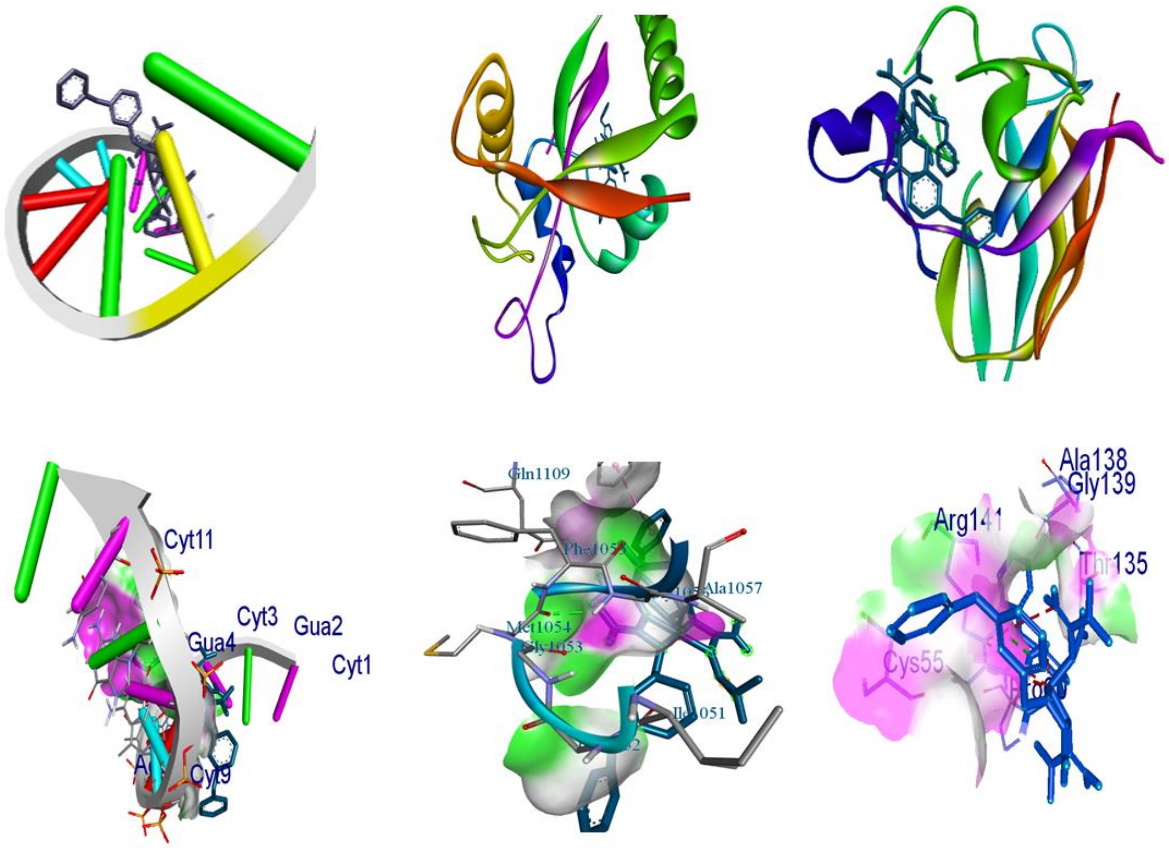

Figure 10. (a) Molecular docking of C-3 complex with 1BNA and 1CB4 (above) **(b)** Active site amino acid residues of (1BNA,4L09, and 1CB4) interactions with C-3 complex (below).

Table 4. Docking score of ligand (HL) and complexes C-1, C-2 and C-3.

Compound	**Binding energy(kcal/mol)**		
	1BNA	4L09	1CB4
HL	-6.5	-8.0	-7.5
C-1	-6.9	-7.9	-7.8
C-2	-7.4	-8.3	-8.1
C-3	-7.0	-8.1	-7.9

3.9. DNA binding studies.

3.9.1. Electronic absorption titrations.

Electronic absorption spectroscopy is a technique used to determine the binding interaction of metal complexes with DNA. The absorption spectra of Cu(II) and Ni(II) complex in the presence of CT-DNA is shown in Fig 11 and Fig 12, respectively. The binding constant K_b for the complex has been determined from the plot of [DNA]/(ϵa-ϵf) versus [DNA], using equation (eq-1), and was found to be 3431.01 M^{-1} and 1440.84 M^{-1}, respectively [39].

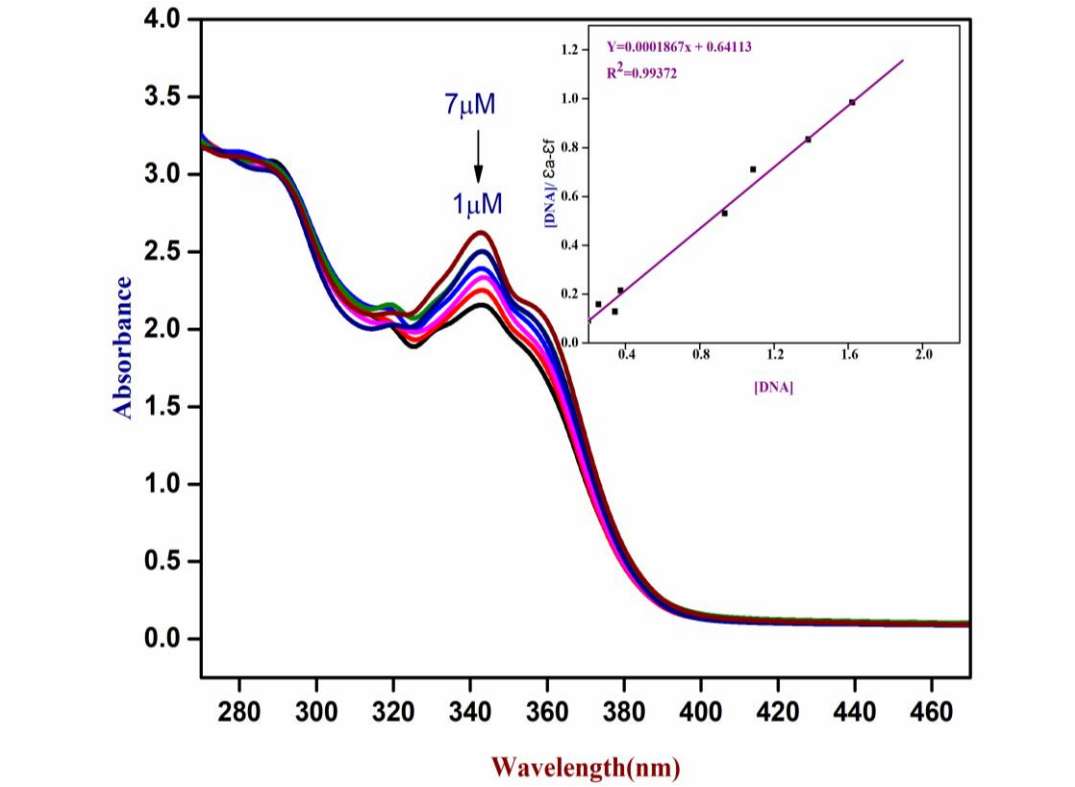

Figure 11. Absorption spectra of C-2 complex in the presence of CT-DNA in tris-HCl buffer (pH=7.4); Inset: The plot of [DNA]/(***ϵ***a-***ϵ***f) versus [DNA].

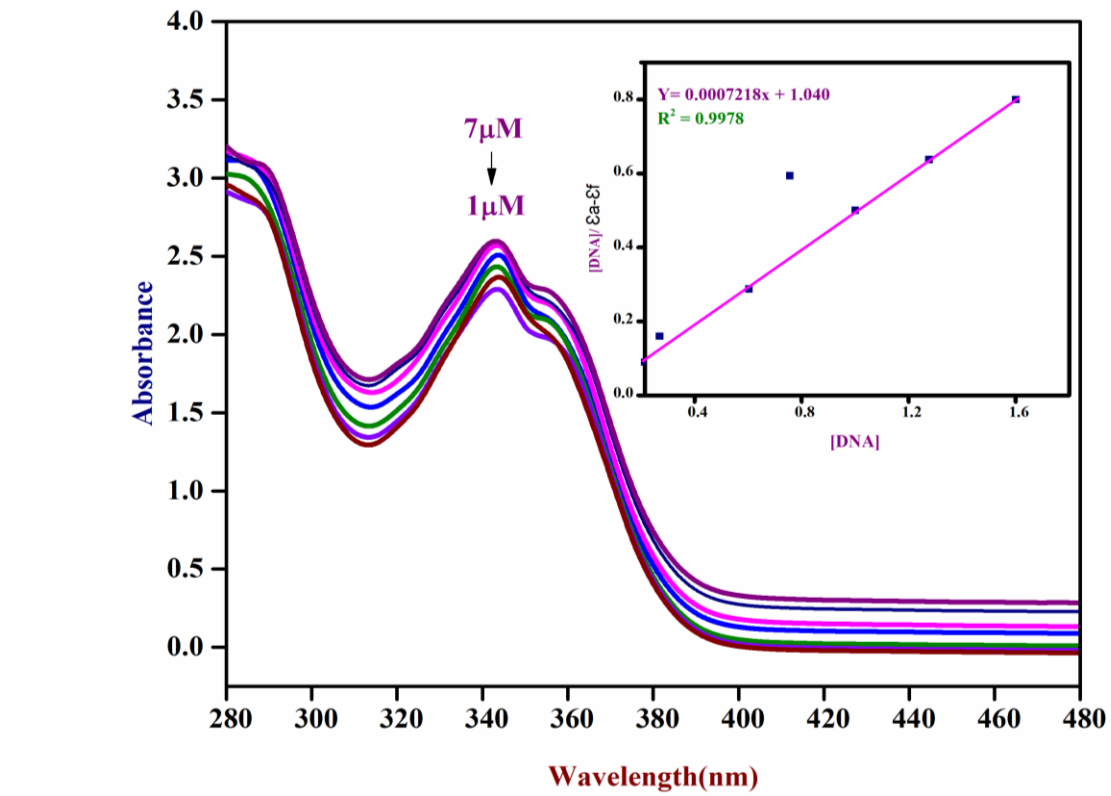

Figure 12. Absorption spectra of C-3 complex in the presence of CT-DNA in tris-HCl buffer(pH=7.4); Inset: The plot of [DNA]/(***ϵ***a-***ϵ***f) versus [DNA].

3.9.2. Fluorescence spectroscopic studies.

The fluorescence experiments were carried out to explore the interaction between ligands and complexes with CT-DNA. The fluorescence spectra of the ligand showed no change in intensity upon the addition of CT-DNA. The fluorescence spectra of the complexes exhibited major peaks at 500 and 510 nm, respectively [Fig-13 and Fig-14]. Initially, the low fluorescence intensity was observed due to quenching by the solvent molecule, and gradually the intensity increased when it binds with DNA. On increasing the concentrations of metal complexes, the emission intensity decreased slowly. The fluorescence emission intensities at 500 and 510 nm (excitation at 350 and 340nm) diminished with the increase of complex concentration. The quenching of fluorescence intensity of complexes by binding with CT-DNA was further used to determine the binding constant (Kb) from the plot of F_0/F versus [Q] using the following equation [eq-3] and was found to be 7.282×10^3 M^{-1} and 5.750×10^3 M^{-1} and the Stern-Volmer quenching constant (ksv), was obtained from the plot of log $[(F_0-F)/F]$ versus log[Q], [Fig 15 and Fig 16] using the following equation (eq-4) and were found to be 2.029×10^3 and 2.001×10^3. These results indicate that Cu (II) complex binds to DNA by intercalation mode more efficiently than Ni (II) complex [40].

$$\frac{F0}{\Delta F} = \frac{1}{fa} + \frac{1}{faKa}[Q] \quad (3)$$

$$\log\left(\frac{F0-F}{F}\right) = \log k_b + n\log[Q] \quad (4)$$

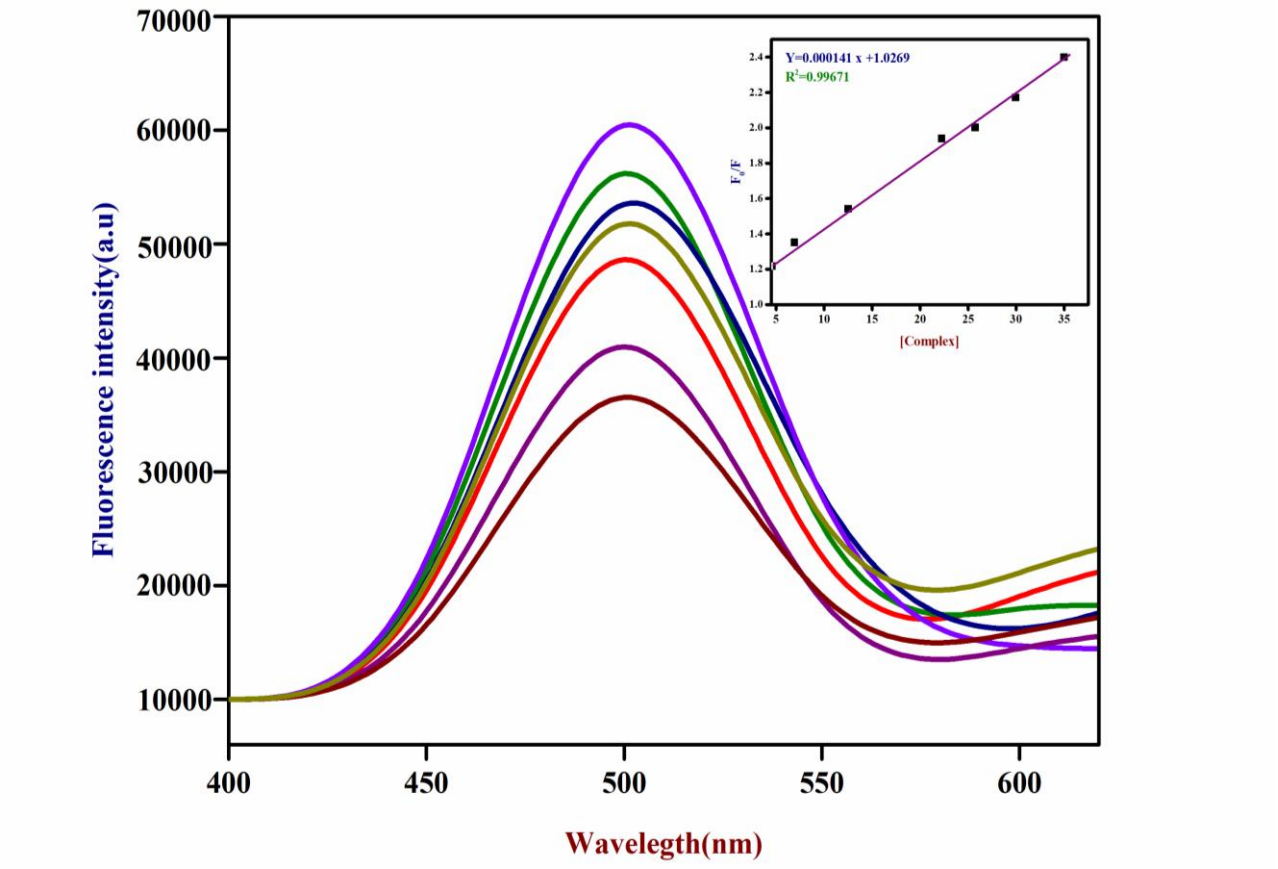

Figure 13. Emission spectra of C-2 complex in the presence of CT-DNA in tris-HCl buffer(pH=7.4)[e_{xec}=350nm; λ_{ems}=500nm]; Inset: The plot of F_0/F v/s [Q].

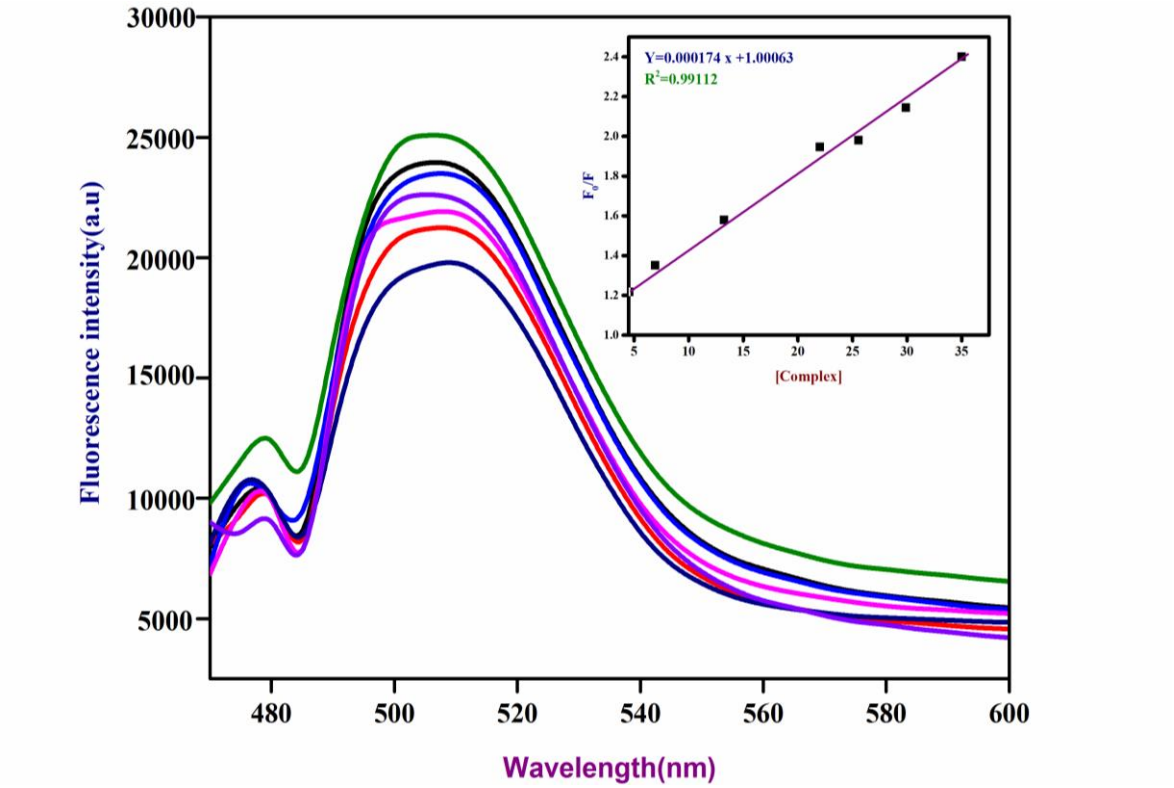

Figure 14. Emission spectra of C-3 complex in the presence of CT-DNA in tris-HCl buffer (pH=7.4) [λ_{exc}=340nm; λ_{ems}=510nm]; Inset: The plot of F_0/F v/s [Q].

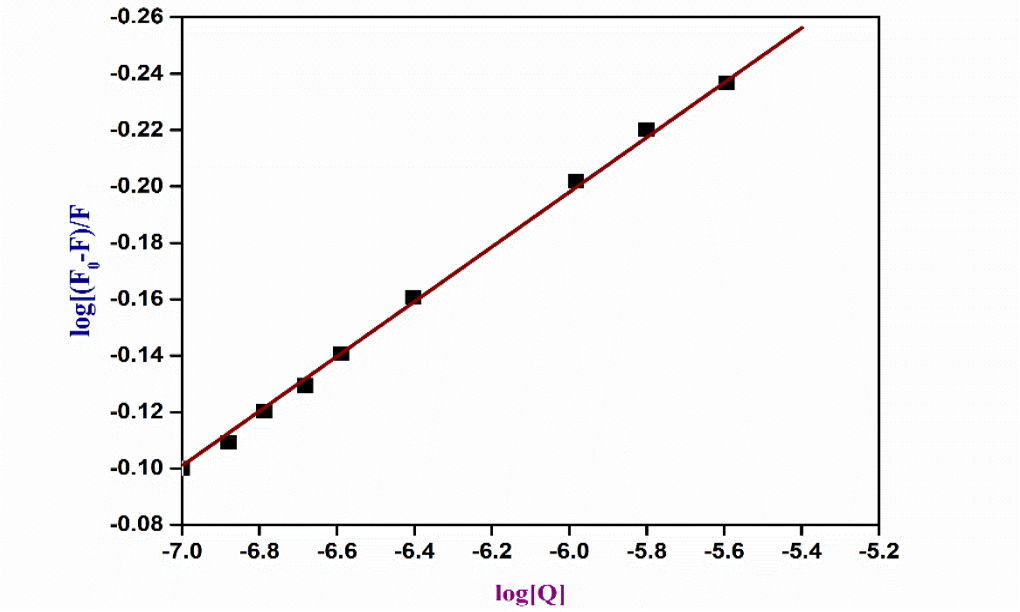

Figure 15. A plot of log[(F_0-F)/F] versus log[Q].

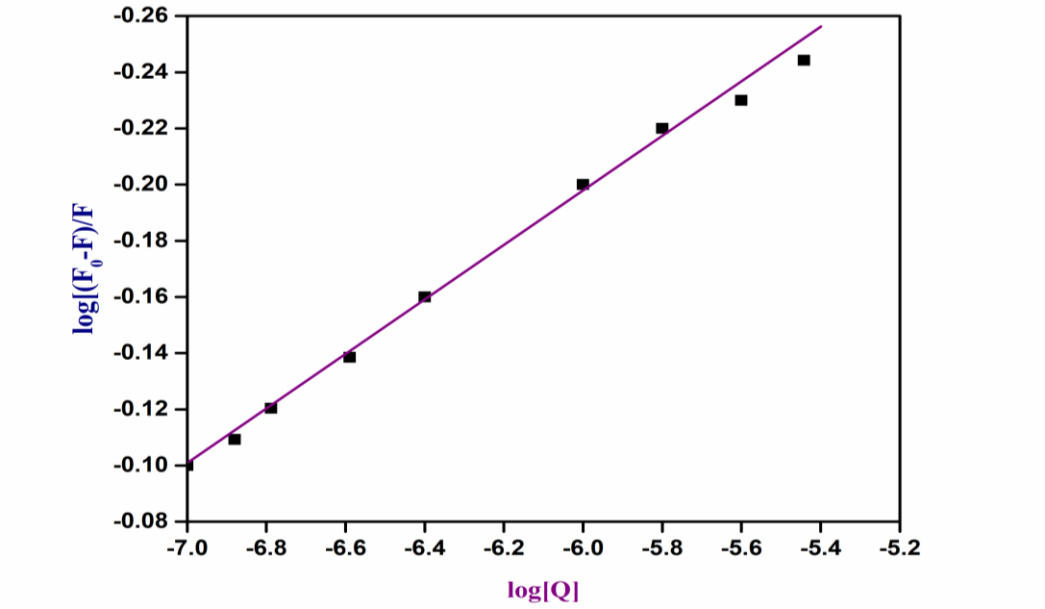

Figure 16. A plot of log[(F_0-F)/F] versus log[Q].

3.10. Pharmacological studies.

3.10.1. Evaluation of antioxidant activity.

The synthesized compounds showed lower scavenging activity compared to the standard. The antioxidant property of the ligand (HL) and its metal complexes is expressed as IC_{50} values depicted in Table 5. Among the synthesized compounds, Cu(II) and Ni(II) complexes showed the highest antioxidant activity leading to a lower IC_{50} value. since the substituents /groups electron-donating and electron-withdrawing groups] play a significant role in antioxidant activity. Fig 17 and Table 5, describe the inhibitory effects of HL and its metal complexes[C-1 to C-3] [41,42].

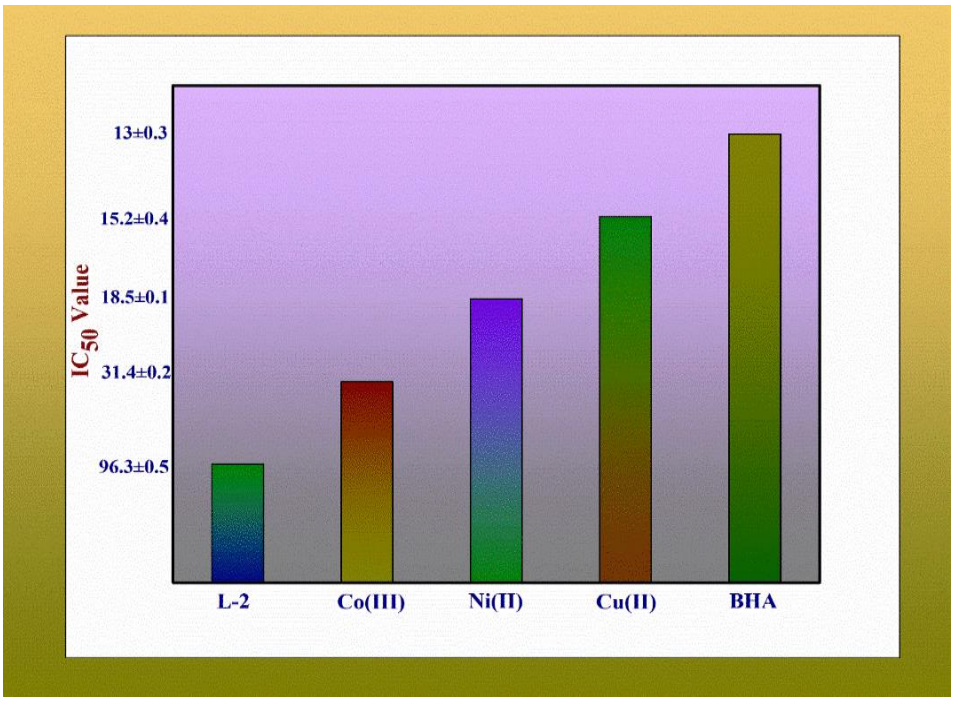

Fig 17. IC_{50} inhibitory concentration of ligand (HL) and its metal complexes (C-1 to C-3) for 50% of DPPH radical.

Table 5. 50% Inhibitory concentrations of (IC_{50}) radical scavenging activity of ligand (HL) and metal complexes C-1, C-2 and C-3.

Sl.No	Compound	IC_{50}
1	HL	96.3±0.5
2	C-1	31.4± 0.2
3	C-2	15.2±0.4
4	C-3	18.5 ±0.1
5	BHA	13±0.3

3.10.2. Antimicrobial activity.

The antimicrobial activity tests were conducted using bacteria and fungal strains. The results were recorded as shown in Table 6. It is inferred that the Schiff base ligand and its metal complexes inhibited the growth of *B. subtitlis*, *E.coli* and *S. aureus* [43].

The susceptibility zones were measured in diameter(mm), and these zones were the clear zones around the discs killing the bacteria. The ligand (HL) and metal complexes individually exhibited varying degrees of inhibitory effects on the growth of tested bacterial species. The metal complexes showed more antibacterial activity than the ligand (HL) [44]. All of the investigated compounds caused greater inhibition zones compared to the standard shown in Fig 18 and tabulated in Table 6 [45].

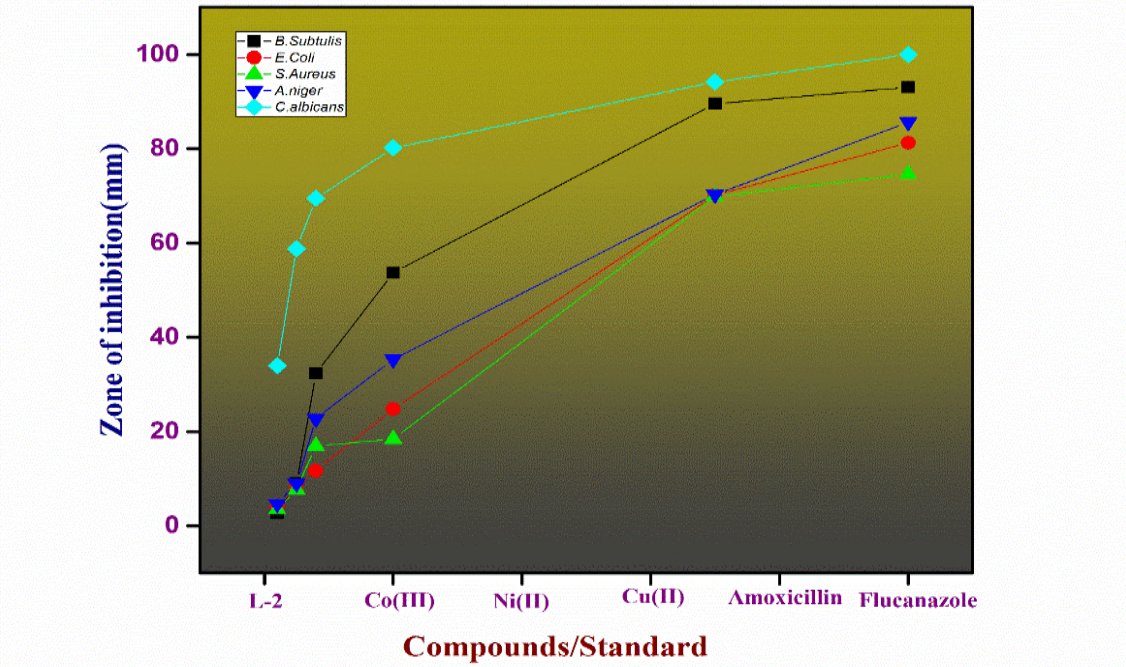

Figure 18. Graphical representation of the antimicrobial activity of HL and its metal complexes C-1, C-2 and C-3.

Table 6. Antimicrobial activity of ligand (HL) and its complexes C-1, C-2 and C-3.

Compound	Zone of Inhibition				
	Bacteria			Fungi	
	B. subtilis	*E. coli*	*S. aureus*	*A. niger*	*C. albicans*
HL	10	12	12.5	09	08
C-1	23	20	17	17	13
C-2	24	23	20	19	17
C-3	22	19.5	17	18	16
Amoxicillin	28	23	25	-	-
Fluconazole	-	-	-	41	36

4. Conclusion

In the present study, Schiff base[HL] and its metal complexes of Co(III),Cu(II), and Ni(II) were synthesized and characterized by physicochemical methods. Elemental analysis reveals that the complexes have a ligand-to-metal ratio (2:1). FT-IR spectra support the coordination of ligand-to-metal through azomethine nitrogen and nitrogen of the amine group. ^{1}H-NMR, ^{13}C-NMR, LC-MS, and FT-IR data support the structure of ligand (HL) and the complexes. TGA depicts the degradation path and stability of the complexes formed. The presence of azomethine and amine groups in the ligand enhanced the antioxidant activity of the complexes. The antibacterial and antifungal activities presented in this paper infer that the copper complex showed the highest degree of antibacterial and antifungal activities compared to cobalt and nickel complexes. Molecular docking studies indicate that Cu(II) complex binds more effectively with p53 cancer mutant protein than DNA and hydrolase enzyme.

Acknowledgment

The author M Prema thankful to the UOM-OBC cell for awarding the fellowship and also extending thanks to the Institute of Excellence, Vijnan Bhavan, Mysuru, and IIT Bombay for Instrumental facilities.

REFERENCES

1. Yadav, G.; Mani, J.V. Green Synthesis of Schiff Bases using Natural Acid Catalysts. *International Journal of Science and Research* **2015**, *4*, 121-127.
2. Shekekhawat, A.S.; Singh, N.P; Chundawat, N.S. Synthesis, Characterization and Biological Activities of Schiff Base Metal Complexes Derived from Hydroxy Trizene and Aromatic Aldehyde. *Journal of Scientific Research* **2022**, *14***,** 387-394 http://dx.doi.org/10.3329/jsr.v14i1.54814.
3. Raczuk, E.; Dmochowska,B.; Friertek, J.S. and Madaj, J. Different Schiff Bases- Structure, Importance and Classification. *Molecules* **2022**, *27*, 787, https://doi.org/10.3390/molecules27030787.
4. Xavier, A.; Srividhya, N. Synthesis and Study of Schiff Base Ligands. *Journal of Applied Chemistry (IOSR-JAC)* **2014**, *7*, 06-15.
5. Nawaz, N.; Ahmad, I.; Darwesh, N.M.; Wahab, A.; Rahman, S.U.; Sajid, A.; Khan, F.A.; Khan, S.B.; Patching, S.G. and Uddin, K. Synthesis, Characterization and Antioxidant Activity of Nickel(II)Schiff Base Complexes Derived from 4-(Dimethylamino)benzaldehyde. *J. Chem. Soc. Pak* **2020**, *42*, 238 -242.
6. Bereber,N.; Arslan,M. Preparation and Characterization of Some Schiff Base Compounds .*ADYU J SCI*, **2020**, *10*,179-188, https://doi.org/10.37094/adyujsci.633080.
7. Ashraf, M.A.; Mahmood, K.; Wajid, A. Synthesis, Charaterization and Biological Activity of Schiff Bases. *International Conference on Chemistry and Chemical Process* **2011**, *10*, 1- 7.
8. Borase, J.N.; Mahale, R.G.; Rajput, S.S.; Shirsath, D.S. Design, Synthesis and biological evaluation of heterocyclic methyl substituted pyridine Schiff base transition metal complexes. *SN Applied Sciences* **2021,** *3*, 1-13 https://doi.org/10.1007/s42452-021-04144-z.
9. Vijayalakshmi, M. Synthesis and Characterization of some Transition Metal Complexes of Schiff Base Derived From 2,4-Dihydroxybenzaldehyde. *Iranian Journal of Pharmaceutical Scences* **2019**, *15*, 29-40.
10. Ommenya, F.K.; Nyawade, E.A.; Andala, D.M. and Kinua, J. Synthesis, Characterization and Antibacterial Activity of Schiff Base, 4-chloro-2-{(E)-[(4-fluorophenyl) imino]methyl}phenol Metal(II) Complexes. *Journal of Chemistry* **2020,** 1-8, http://doi.org/10.1155/2020/1745236
11. Saxena, A. Synthesis and Characterization of Schiff base salicylaldehyde and thiohydrazones and its metal complexes. *Advances in applied Science Research* **2013**, *4*, 152-154.
12. Chaudhary, N.K. Bibechana A. Multidisciplinary. *Journal of Science, Technology and Mathematics* **2013**, *9*, 75-80.
13. Tajudeen, S.S.; Geetha, K. Schiff Base-Copper(II)Complexes: Synthesis, Spectral studies and Antitubercular and Antimicrobial Activity. *Indian Journal of Advances in Chemical Science* **2016**, *4*,40-48.
14. Joseyphus, R.S.; Shiju, C.; Joseph, J.; Dhanaraj, C.J.; and Bright, K.C. Synthesis and Characterization of Schiff base metal complexes derived from imidazole-2-carboxaldehyde with L-phenylalanine. *Der Pharma Chemica* **2015**, *7* , 265-270.

15. Dileep Kumar, A.; Naveen, S.; Vivek, H.K.; Prabhuswamy, M.; Lokanath, N.K.; Ajay Kumar, K. Synthesis, crystal and molecular structure of ethyl 2-(4-chlorobenzylidene)-3-oxobutanoate: Studies on antioxidant, antimicrobial activities and molecular docking. *Chemical Data Collections* **2016**, 5, 36-45, https://doi.org/10.1016/j.cdc.2016.10.002.
16. Maryam Hosseini, Wanqui Chen, Daliao Xiao and Charles Wang *Precision Clinical Medicine* **2021**, *4*, 1-16, https://doi.org/10.1093/pcmedi/pbab001.
17. Sharafalddin, A.A.; Emwas, A.H.; Jaremco, M.; Hussien, M. A. Practical and Computational Studies od Bivalence Metal Complexes of Sulfaclozine and Biological Studies. *Front Chem* **2021**, *9*, 1-16, https://doi.org/10.3389/fchem.2021.644691.
18. Abu, F.; Che Norma Mat Taib, Mohammad Aris Mohd Moklas and Sobri Mohd Akhir *Evidence- Based Complementary and Alternative Medicine* **2017**, 1-9, https://doi.org/10.1155/2017/2907219.
19. Ozlem, O.; Perihan, G.; Yaprak Dilber, S. d.; Mustafa. ARK *Journal of Science* **2020**, *33*, 646-660, https://doi.org/10.35378/gujs.654598.
20. Saranya, J. and Santha Lakshmi, S. In vitro antioxidant, antimicrobial and larvicidal studies of Schiff base transition metal complexes. *Journal of Chemical and Pharmacrutical Research* 2015, *7*, 180-186, https://www.jocpr.com/abstract/in-vitro-antioxidant-antimicrobial-and-larvicidal-studies-of-schiff-base-transition-metal-complexes-3424.html.
21. Weigand, I.; Hilpert, K.; Hancock, R.E.W. agar and broth dilution methods to determine the minimal inhibitory concentration (MIC)of antimicrobial substances. *Nature Protocol*, **2008**, *3*, 163-175.
22. Chavez, F.A.; Nguyen, C.V.; Olmestead, M. M.; Mascharak, P.K. Synthesis,Properties and structure of a stable Cobalt(III)Alkyl peroxide complex and its role in the oxidation of cyclohexane. *Inorganic Chemistry* **1996**, *35*, 6282-6291, https://doi.org/10.1021/ic960500m.
23. Pogany, L.; Monol, J.; Gal,M.; Salitros, I.; Boca, R.; Four cobalt(III)schiff base complexes-structural, spectroscopic and electrochemical studies. *Inorganica Chimica Acta*, **2017**, *462*, 23-29, https://doi.org/10.1016/j.ica.2017.03.001.
24. Jisha, M. J.; Sobana Raj, C.I. Synthesis and characterization of Schiff base complexes of Cu(II), Ni(II), Co(II) complexes of Schiff base derived from furan 3- carboxaldehyde and 3- amino pyridine. *International Journal of Scientific and Research Publications* **2017**, *7*, 10-19.
25. Bartyze, A. Synthesis, thermal study and some properties of N_2O_4—donor Schiff base and its Mn(III), Co(II), Ni(II), Cu(II) and Zn(II) complexes. *J Therm Anal Calorim* **2016**, *127*(3), 1-15, https://dx.doi.org/10.1007/s10973-016-5804-0.
26. Dar, U.A.; Gawali, S. S.; Shinde, D.; Bhand, B. and Satpute, S. Thermal and Spectral Studies of Transition Metal Complexes of 2-Bromo-3-Hydroxynaphthalene-1,4-Dione: Evaluation of Antibacterial Activity Against Six Bacterial Strains. *Engineered Science* **2021**, *15*, 105-115, https://dx.doi.org/10.30919/es8D492.
27. Kaya, Y.; Mutlu, H.; Rez, G. Uv-Vis Spectra and Fluorescence Properties of Two Iminooxime Lignds and Their Metal Complexes: Optical Band Gap. *G.U. Journal of Science* **2010**, *23*, 13-18.
28. Akinyele, O. F.; Fakola, E. G.; Durosinmi, L. M.; Ajayeoba, T. A.; Ayeni, A. O. Synthesis and Characterization of Heteroleptic Metal Complexes of Isoniazid and Metformin. *Ife Journal of Science* **2019**, *21*, 1-7, https://dx.doi.org/10.4314/ijs.v21i3.15.
29. Kotkar, S.N. and Juneja, H.D. Synthesis, Characterization and Antimicrobial Studies of N, O Donor Schiff Base Polymeric Complexes. *Journal of Chemistry* **2013**, 2013, 1-5, http://dx.doi.org/10.1155/2013/479343.
30. Abou Melha, K. S.; Al-Hazmi, G. A.; Althagafi, I.; Alharbi,A.; Keshk, A.A.; Shaaban, F. and El-Metwaly, N. Spectral, Molecular Modeling, and Biological Activity Studies on New Schiff's Base of Acenaphthaquinone Transition Metal Complexes. *Bioinorg Chem Appl.* **2021**, *2021*, 1-15, https://doi.org/10.1155/2021/6674394.
31. Neha, M.; Biplab, M. TGA Analysis of Transition Metal Complexes Derived from Phenothiazine. *International Journal of Engineering and Scientific Research* **2018**, *6*, 47-57.
32. Gaber, A.; Belal, A. A. M.; El-Deen, I.M.; Hassan, N.; Zakaria, R.; Alsanie, W.F.; Naglah, A.M.; Refat, M.S. Synthesis, Spectroscopic Characterization and Biological Activities of New Binuclear Co(II), Ni(II), Cu(II) and Zn(II) Diimine Complexes. *Crystals* **2021**, *11*, 1-17, https://doi.org/10.3390/cryst11030300.
33. Refat, M.S.; Altahi, T.A.; Al-Haza, I, G. H.; Al-Humaidi, J.Y. Synthesis, Characterization, Thermal Analysis and Biological Study of New Thiophene Derivative containing o-Aminobenzoic acid ligand and its Mn(II), Cu(II) and Co(II) Metal Complexes. *Bull. Chem. Soc. Ethiop.* **2021**, *35*, 129-140, https://doi.org/10.4314/bcse.v35i1.11.
34. Begum, T.N.; Raju, J.; Sreeramulu, J. Synthesis and biological evaluation of some new Schiff Base metal complexes. *J. Chem. Pharm. Res.* **2014**, *6*, 1198-1209.

35. El-Ghamry, M.A.; Elzawawi, F.M.; Aziz, A.A.A.; Nasir, K.M.; El-Wafa, S.M.A. New Schiff base ligand and its novel Cr(III), Mn(II), Co(II), Ni(II), Cu(II), Zn(II) Complexes: spectral investigation, biological applications and semiconducting properties. *Scientific Reports* **2022**, *12*,1-21, https://doi.org/10.1038/s41598-022-22713-z.
36. Noureddine. O.; Issaoui, N.; Garfaoui, S.; Dossary, O.A.; Marouani, H. Quantum chemical calculations, spectroscopic properties and molecular docking studies of novel piperazine derivative. *Journal of King Saud University-Science* **2021**, *33*,101283, 1-15, https://doi.org/10.1016/j.jksus.2020.101283.
37. Melavanki, R.; Sarma, K.; Muttannavar, V.T.; Kusanaur, R.; Katagi, K.; Patra, S.M.; Umapathy, S.; Sadasivuni, K.K.; Shelar, V.M.; Singh, D.; Patil, N.R.; Varsha, V.K. Quantum chemical computations, fluorescence spectral features and molecular docking of two biologically active heterocyclic classof compounds. *Journal of Photochemistry and Photobiology, A:* Chemistry **2021**, *404*, 1-18, https://doi.org.10.1016/j.jphotochem.2020.112956.
38. Almarhoon, Z.M.; Al-Onazi, W.A.; Althaman, A.A.; Al-Mohaimeed, A.M.; Al-Farraj, E.S. Synthesis, DNA Binding, and Molecular Docking Studies of Dimethylaminobenzaldehyde-Based Bioactive Schiff Bases. *Journal of Chemistry* **2019,** 1-14, http://doi.org/10.1155/2019/8152721.
39. Wu, H.; Sun, T.; Li, K.; Liu, B.; Kou, F.; Jia, F.; Yuan, J.; Bai, Y. Synthesis, Crystal structure and DNA Binding Studies os a Nickel(II) Complexe with the Bis(2-benzimidazolymethyl)amine Ligand. *Bioinorganic Chemistry and Applications* **2012**, *2012*, 1-7, https://doi.org/10.1155/2012/609796.
40. Vamshikrishna, N.; Pradeepkumar, M.; Ramesh, G.; Ganji, N.; Daravath, S.; Shivaraj. DNA interactions and biocidal activity of metal complexes of benzothiazole Schiff bases: Synthesis, Characterization and validation. *Journal of Chemical Science* **2017**, *129*, 609-622, https://doi.org/10.1007/s12039-017-1273-7.
41. Yakan, H. Preparation, structure elucidation and antioxidant activity of new bis(thiosemicarbazone)derivatives. *Turkish Journal of Chemistry* **2020**, *44*, 1085-1099, https://doi.org/10.3906/kim-2002-76.
42. Jirjees, V.Y.; Suleman, V.T.; Ahmed, S.D.; Al-Hamdani, A.A.S. Determination of antioxidant activity for metal ions complexes. *Journal of University of Duhok* **2020**, *23*, 41-50, https://doi.org/10.26682/sjuod.2020.23.1.5.
43. Njimoh, D.L.; Assob, J. C. N.; Mokake, S. E.; Nyhalah, D. J.; Yinda, C. K. and Sandjon, B. Antimicrobial Activities of a Plethora of Medicinal Plant Extracts and Hydrolates against Human Pathogens and Their Potential to Reverse Antibiotic Resistance. *International Journal of Microbiology* **2015**, *2015*, 1-15, http://dx.doi.org/10.1155/2015/547156.
44. Hossain, M.S.; Zakaria, C.M. and Zahan, M.K. *Journal of Scientific Research* **2017**, *9*, 209-218, http://dx.doi.org/10.3329/jsr.v9i2.29780.
45. Salihovic, M.; Pazalja, M.; Mahmutovic- Dizdarevic, I.; Jerkovic-Mujkic, I.; Sujagic, J.; Spirtovic-Halilovic, S.; Sapcanin, A. *Rasayan Journal Chemistry* **2018**, *11*, 1074-1083, http://dx.doi.org/10.3329/jsr.v9i2.29780

Supplementary materials

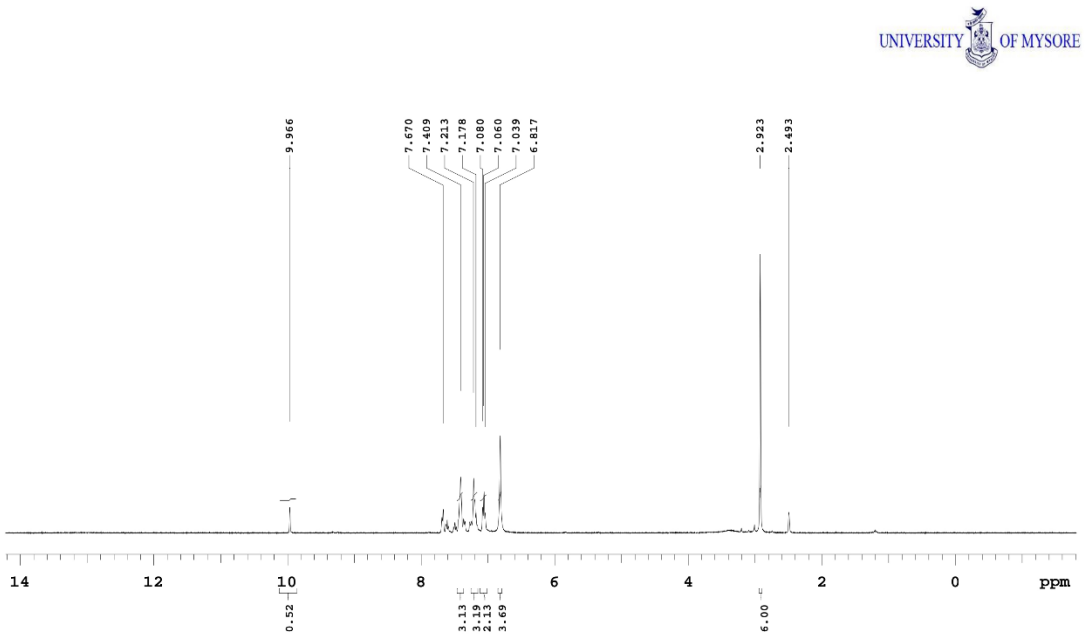

Figure S1. ^{1}H -NMR spectrum of the ligand [HL]

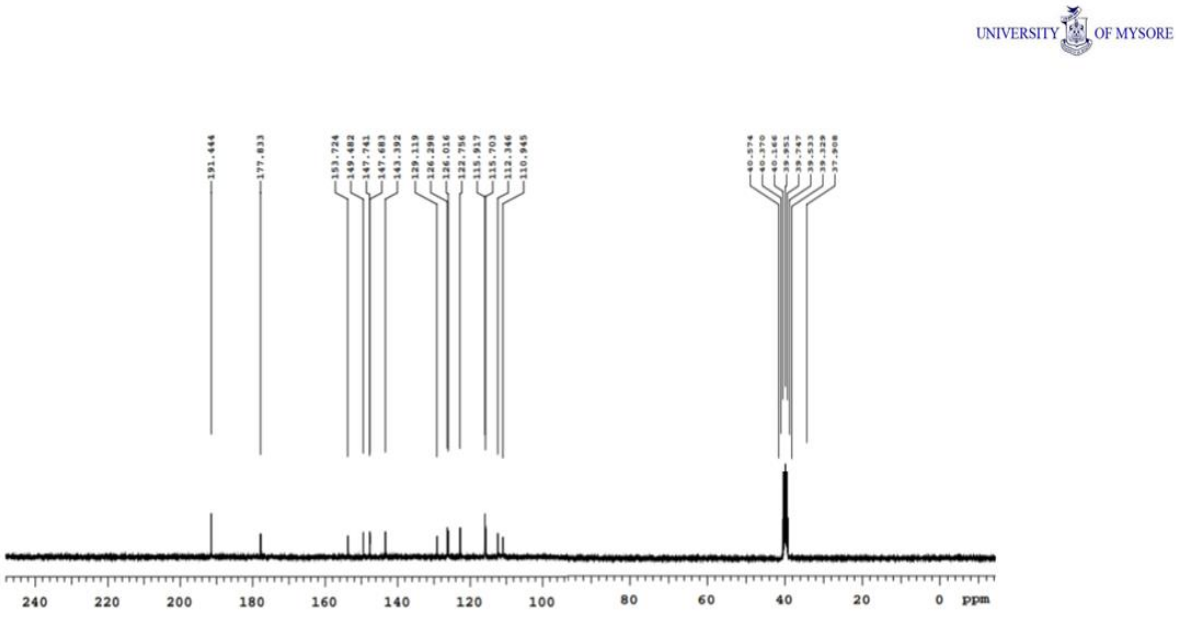

Figure S2. ^{13}C -NMR spectrum of the ligand [HL]

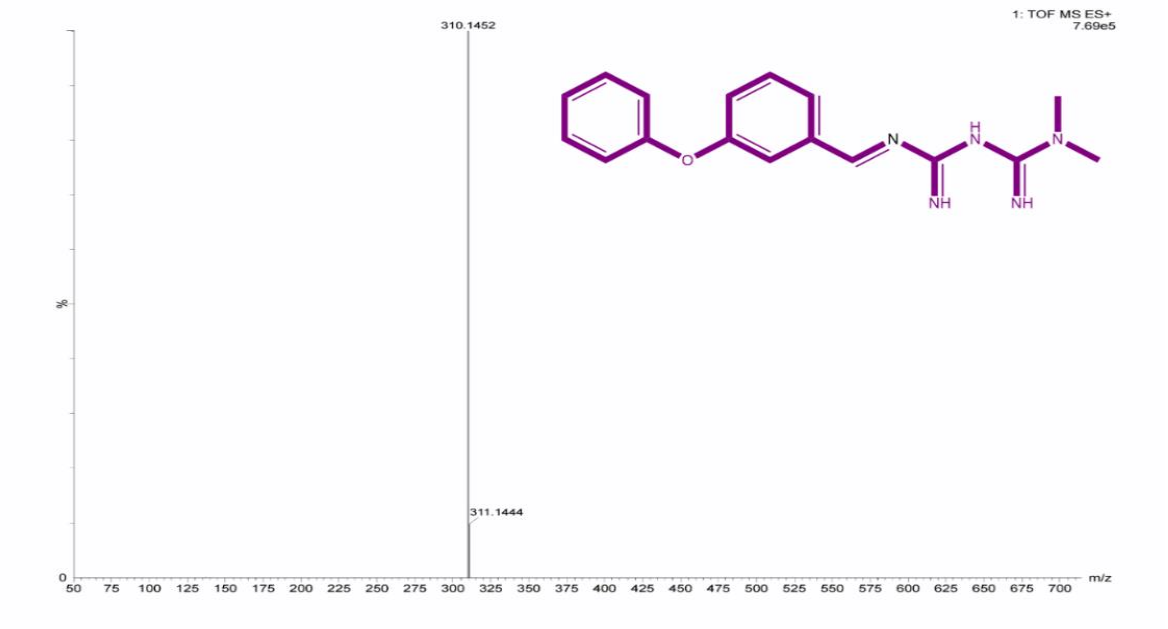

Figure S3. Mass spectrum of the ligand [HL]

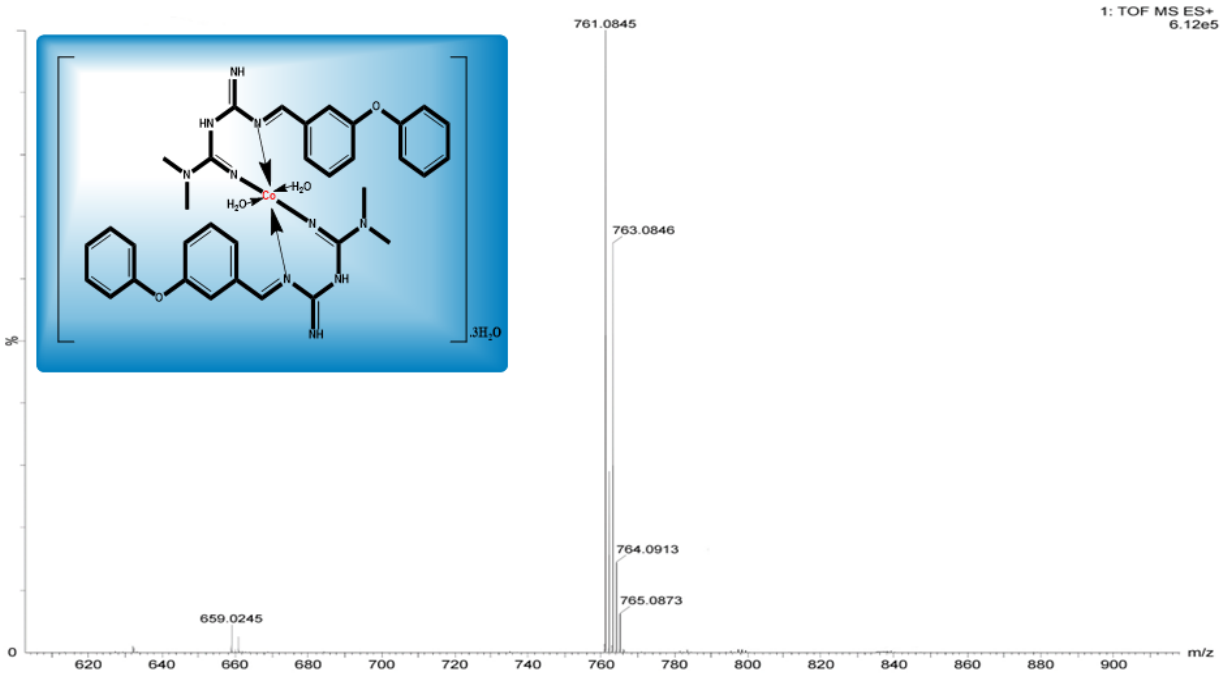

Figure S4. Mass spectrum of Co(III) complex [C-1]

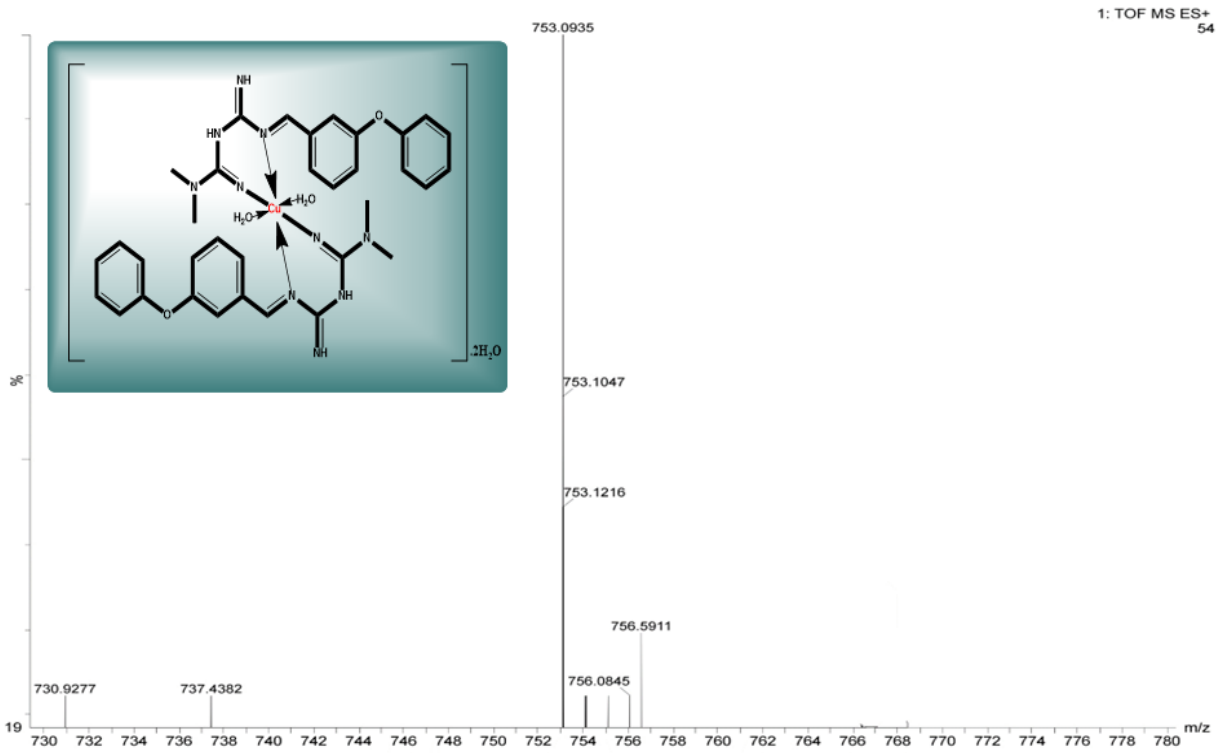

Figure S5. Mass spectrum of Cu(II) complex [C-2]

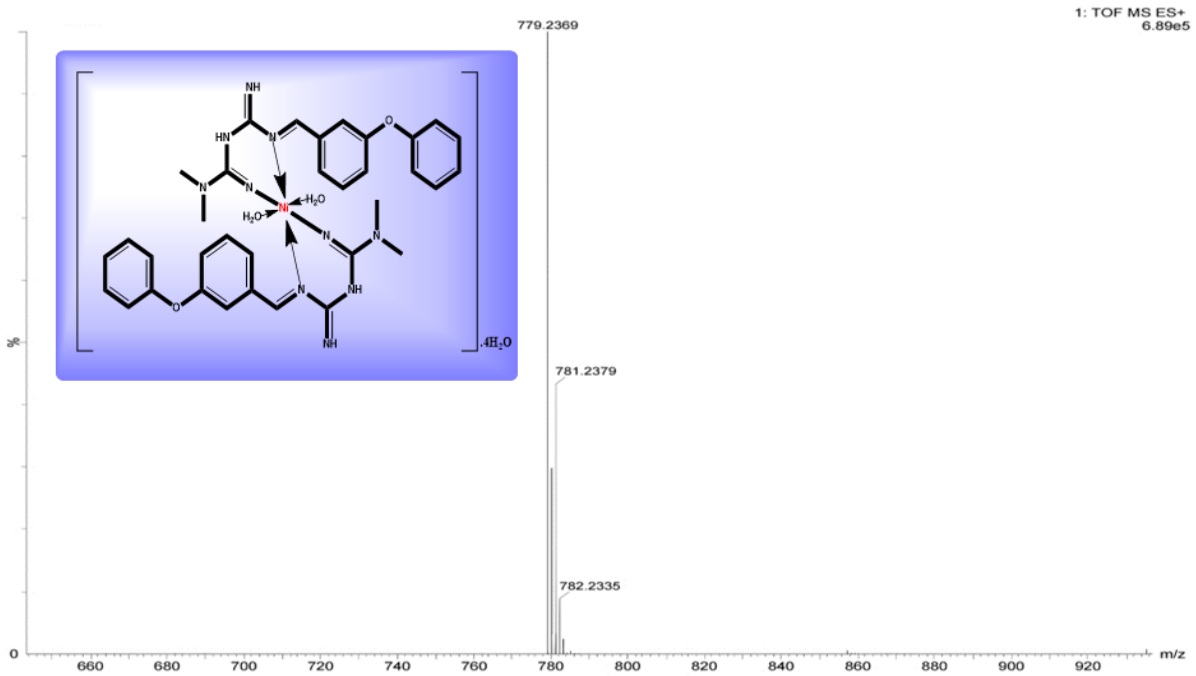

Figure S6. Mass spectrum of Ni(II) complex [C-3]